C.P. No. 1086

C.P. No. 1086

MINISTRY OF TECHNOLOGY

AERONAUTICAL RESEARCH COUNCIL

CURRENT PAPERS

A Theoretical Investigation for Delta Wings with Leading-Edge Separation at Low Speeds

by

R K Nangia and G. J. Hancock

Dept. of Aeronautical Engineering,

Queen Mary College, University of London

LONDON: HER MAJESTY'S STATIONERY OFFICE

1970

PRICE 12s 0d [60p] NET

C.P. No. 1086*
August 1968

A Theoretical Investigation for Delta Wings with Leading-Edge Separation at Low Speeds

- By -
R. K. Nangia and G. J. Hancock,
Dept. of Aeronautical Engineering,
Queen Mary College, University of London

SUMMARY

A non-linear lifting surface theory is postulated which incorporates the leading edge separations, by extending Brown and Michael's slender wing model, but satisfies the Kutta trailing edge condition. Results of a numerical application to a delta wing indicate acceptable trends compared with experimental data.

List of Contents

References/

* Replaces A.R.C.30 608

Notation/

Notation

x, y, z	Rectangular co-ordinate axes system
u, v, w	Perturbation velocity components in x, y, z directions
A	Aspect ratio
$a_{2p+1,q}$	Coefficients in series expansion for $\bar{\delta}_1(\bar{x},\bar{y})$ in equation (58)
$a_y(2p+1,q,\bar{x},\bar{y})$, $a_\delta(2p+1,q,\bar{x},\bar{y})$	Defined in equations (63) and (64)
$aw(2p+1,q,\bar{x},\bar{y})$	Upwash coefficient corresponding to $a_{2p+1,q}$
b	Wing span
c	Wing root chord
C_L	$= \dfrac{L}{\frac{1}{2}\rho V^2 . S_W}$ Lift coefficient
C_N	$= \dfrac{Z}{\frac{1}{2}\rho V^2 . S_W}$ Normal force coefficient
c_p	$= \dfrac{p - p_\infty}{\frac{1}{2}\rho V^2}$ Pressure coefficient
c_{p_ℓ}	$= \dfrac{p_\ell - p_\infty}{\frac{1}{2}\rho V^2}$ Pressure coefficient on wing lower surface
c_{p_u}	$= \dfrac{p_u - p_\infty}{\frac{1}{2}\rho V^2}$ Pressure coefficient on wing upper surface
Δc_p	$= c_{p_\ell} - c_{p_u}$ Loading coefficient
C_m	Pitching moment coefficient about wing apex
d_{tol}	A small tolerance (equations (48), (49))
$F_y(\bar{x})$, $F_z(\bar{x})$, $F(\bar{x})$	Defined in equations (44), (45), (46)
$f_u(\bar{x},\bar{x}_1,\bar{y}_1,\bar{z}_1)$, $f_v(\bar{x},\bar{x}_1,\bar{y}_1,\bar{z}_1)$, $f_w(\bar{x},\bar{x}_1,\bar{y}_1,\bar{z}_1)$	Defined by equations (26), (27), (28)
g_q	Coefficients in series expansion for $\bar{\Gamma}_W(\bar{x})$ in equation (60)

$g_y(q,\bar{x},\bar{y})$, $g_\delta(q,\bar{x},\bar{y})$	Defined by equations (65) and (66)
$gw(q,\bar{x},\bar{y})$	Upwash coefficient corresponding to g_q
k	Slope of the wing starboard leading edge (i.e. $y = kx$)
ℓ	Upper integer limit in series form for $\bar{\Gamma}_W(\bar{x})$ in equation (60)
L	Lift force
m	Upper integer limit in series form for $\bar{\delta}_1(\bar{x},\bar{y})$ in equation (58)
M	Pitching moment about the wing apex
n	Upper integer limit in series form for $\bar{\delta}_1(\bar{x},\bar{y})$ in equation (58)
p,q	Integer indices
S_W	Wing planform in $z = 0$ plane
S_T	Trailing sheet in $z = 0$ plane
$\bar{u},\bar{v},\bar{w}$	u/V, v/V, w/V
$\bar{v}_1(\bar{x},\bar{y}_v(\bar{z}), \bar{z}_v(\bar{x})),\bar{w}_1(\bar{x},\bar{y}_v(\bar{x}), z_v(\bar{x}))$	Induced velocity in $\bar{y},\bar{z}$-directions at the starboard vortex (equations (40), (41))
V	Free stream velocity
X	Force in x-direction
x_{c_p}	Position of centre of pressure
$\bar{x},\bar{y},\bar{z}$	x/c, y/c, z/c
$y_v(x)$, $z_v(x)$	Locations of the starboard vortex
$\Delta\bar{y}_v(\bar{x})$, $\Delta\bar{z}_v(\bar{x})$	Correction to spanwise position and height of the starboard vortex given by equations (50) and (51)
Z	Force in z-direction
α	Incidence
$\beta(y)$	Angle of deflection of streamlines at the trailing edge
$\delta(x,y)$	Trailing 'vorticity', i.e. component of vorticity about the x-direction
$\delta_1(x,y)$	Part of trailing 'vorticity' tending to zero at the leading edge (equation (58))

δ_g/

$\delta_g(x,y)$	Part of trailing 'vorticity' tending to a finite value at the leading edge (equation (5))
$\delta_T(y)$	Trailing vorticity on the wake trailing sheet
$\bar{\delta}(\bar{x},\bar{y})$	$\delta(x/c,y/c)/V$
$\gamma(x,y)$	Bound 'vorticity', i.e. component of 'vorticity' about the y-direction
$\gamma_1(x,y)$	Part of bound 'vorticity' tending to zero at the leading edge } Equation(4)
$\gamma_g(x,y)$	Part of bound 'vorticity' tending to a finite value at the leading edge } Equation(4)
$\bar{\gamma}(\bar{x},\bar{y})$	$\gamma(x/c,y/c)/V$
$\Gamma_W(x)$	Circulation strength of starboard vortex above the wing
$\Gamma_W(c) + \Gamma_T(x)$	Circulation strength of starboard vortex in the wake
$\bar{\Gamma}(\bar{x})$	$\Gamma(x/c)/(c\,.V)$
ρ	Air density
η	$y/(k.x)$

<u>Subscripts</u>

L	Left
R	Right
T	Trailing sheet
Γ	Main vortex (or vortices)
W	Wing planform
u	Upper surface of the wing
ℓ	Lower surface of the wing

I. Introduction

The qualitative flow pattern about a low aspect ratio wing with sharp leading edges at incidence is now well understood. Comprehensive experimental data has indicated the main features of the flow pattern, comprising the rolling up of the vorticity shed from the leading edges into the two primary vortices, the attachment lines, the formation of the secondary vortices, and the characteristic pressure distributions with the high suctions on the upper surfaces induced by the primary vortices.

Theoretical work has been developed along two fronts. One front, based on the slender conical wing approximation, has evolved through the models of Legendre[1], Brown and Michael[2], Mangler and Smith[3], Maskell[4] up to the detailed investigation by Smith[5]; comparison with the relevant experimental pressure data is good. Unfortunately the assumption of slenderness leads to a theory which is independent of Mach number, thus, in general, the theory breaks down at low Mach numbers in the trailing edge regions because the Kutta trailing edge condition is not satisfied. The second front of approach attempts to extend the classical low speed lifting surface theory, incorporating the Kutta trailing edge condition, by including relatively crude representations of the leading edge separations. The works of Gersten[6], Garner and Lehrian[7], and Sacks, Neilson and Goodwin[8] all replace the wing with the usual form of bound vorticity but with some additional system of separated trailing vorticity although the rolling up process is neglected; distributions of loading are not obtained only the overall forces and moments.

In this paper an attempt is made to combine these two approaches, the conventional lifting surface of vorticity in the plane of wing is taken together with a more realistic pattern of rolled up trailing vorticity above the leading edge. This can be regarded as an extension of the slender wing models to non-slender wings in which chordwise effects are significant. Obviously it is not feasible at this stage to generalise Smith's latest work since the numerical work already required in this slender wing case is formidable. So the task of generalising the 'simpler' model of Brown and Michael to non-slender wings is undertaken. It is recognised that the model of Brown and Michael, in which the spiral vortex sheets from the leading edge are replaced by two concentrated line vortices of variable strength with two feeding "cuts" between the line vortices and the respective leading edges, is open to criticism and that quantitative results cannot be regarded with any confidence. But in the opinion of the authors it is essential to keep the model as simple as possible since it is expected that numerical work will be extensive. In any case the extension of the Brown and Michael's model will be an advance on the existing work. Even with this limited objective the authors have not come up with a programme which can be plugged into the nearest computer, all that has been achieved is a grasp of what the solution entails and the order of magnitude of numerical effort which is required to give reliable quantitative answers relative to the assumed model.

The flow past a finite thin symmetrical delta wing at incidence with separations all along the leading edge is considered. The aim is to extend the Brown and Michael model to include the Kutta trailing edge condition. The basic model is shown in Fig. 1.

The origin of Cartesian co-ordinates, x, y, z is placed at the apex of the wing and the x-axis is taken to pass through the mid-point of the trailing edge. The strength of the starboard line vortex above the wing is denoted by $\Gamma_W(x)$; and taking the axis of the 'cut' in the plane normal to the wing surface the strength of the 'cut' is denoted by $\frac{d\Gamma_W(x)}{dx}$. The vortex

system/

system on the port side is equal and opposite to the starboard system.

The wing surface S_W is to be replaced by a vortex sheet with distributions of bound 'vorticity' $\gamma(x,y)$ and trailing 'vorticity' $\delta(x,y)$. To satisfy the boundary condition that the upwash just off the leading edge is finite the vorticity component parallel to the leading edge tends to zero as $d^{1/2}$, where d is the distance from the leading edge, then the vorticity component normal to the leading edge at the leading edge represents the strength of the 'cut' $\left(\text{i.e. } \dfrac{\partial\Gamma_W(x)}{\partial x}\right)$

The wake aft of the trailing edge comprises the vorticity shed from the wing trailing edge together with the two convected separated leading edge vortex systems.

Because of the velocity field induced by the separated leading edge line vortices, the vorticity shed from the trailing edge feeds into the downstream discrete vortices. This aspect is included in the present model by introducing an approximate form of the wake shown in Fig. 1. Filaments of vorticity which leave the trailing edge are deflected outwards at an angle $\beta(y)$ under the influence of the spanwise velocity field due to the main leading edge vortices. Downstream of the trailing edge it is assumed that these vortex lines remain straight at the same angle until reaching the side edges of the wake ($|y| = s$) where they are immediately convected into the main vortices via cuts joining the side edges of the wake to the main trailing vortices. This model crudely represents the absorption of the vorticity shed from the trailing edge into the leading edge vortices and gives far downstream a completely rolled up trailing vortex system. The rolling up process has necessarily had to be incorporated into the present non-linear theory; the concept of a non-rolled up trailing vortex sheet extending from the trailing edge to infinity is only feasible and consistent within the framework of a linear theory.

A numerical collocation method is developed. The wing vorticity $\delta(x,y)$ on S_W is expressed as a double Fourier series in terms of 20 unknown coefficients, while the strength of the leading edge vortex is expressed a fifth order polynomial with 5 unknown constants. For a specified position of the leading edge vortex the complete vorticity system (i.e. both $\delta(x,y)$ and $\Gamma_W(x)$) can be evaluated in terms of these 25 unknowns. The upwash condition is satisfied at 20 points on the wing and the condition of zero load at the trailing edge is satisfied at 5 discrete points. These last five equations are non-linear since there is an interaction between the wing vorticity and the leading edge vortices. To cope with this difficulty a method requiring a double iteration procedure is developed. First the position of the leading edge vortex is assumed; the variation of the shedding angle $\beta(y)$ of the trailing sheet vorticity from the trailing edge is assumed across the span, and the appropriate equations, which are now linear, are solved; it is feasible to recalculate the shedding angle of the trailing sheet vorticity and this aspect can be iterated out further. Based on the results obtained the condition of zero force on the leading edge vortex system leads to a new position of the leading edge vortex and the whole process can be repeated. As will be discussed later, one of the major difficulties is that the two iterations cannot be accomplished one within the other, it is best to let them develop in parallel. These difficulties are discussed from the experience of a worked example in Section III. In this worked example the intricacies of convergence have not been completely unravelled, however the theoretical results obtained are encouraging and the trends compare favourably with experimental data.

II./

II. Mathematical Formulation

II.1 Model and axes

For a delta wing in a low speed flow of velocity V the origin of the rectangular set of Cartesian co-ordinates x,y,z is located at the wing vertex. The x-axis is taken to pass through the mid-point of the trailing edge as shown in Fig. 1. The dimensions of the delta wing are denoted by the root chord c, span $2s\,(=2kc)$ and the leading edges are given by $y = \pm k.x$.

An uncambered wing surface at an incidence α is defined by $z_W(x,y) = 0$. The wing surface area is denoted by S_W. The extension aft of the trailing edge on the plane $z = 0$ of the wake strip $(x \geq c, |y| \leq s)$ is denoted by S_T. These definitions of S_W and S_T differ from those in conventional linear theory where both S_W and S_T are usually projections on a plane parallel to the free stream.

As mentioned previously the strength of the starboard vortex over S_W is denoted by $\Gamma_W(x)$, positive anti-clockwise, and its position is denoted by $(x, y_v(x), z_v(x))$. The strength of the port vortex is given by $-\Gamma_W(x)$ (in anti-clockwise sense) and its position in this symmetrical problem by $(x, -y_v(x), z_v(x))$. Aft of the trailing edge, $x \geq c$, above S_T, the strength of the starboard vortex will be written as $\Gamma_W(c) + \Gamma_T(x)$.

Since each of these line vortices increases in strength downstream of the origin, the feeding of these line vortices is accomplished by the introduction of 'cuts'. In the region of the wing S_W each of the cuts extends from the leading edge to the neighbouring line vortex; in the region of the trailing sheet S_T the cut extends from the side edge of S_T to its neighbouring line vortex. The strength of the 'cuts' are equal to

$$\frac{\partial \Gamma_W(x)}{\partial x} \qquad 0 \leq x \leq c$$

and

$$\frac{\partial \Gamma_T(x)}{\partial x} \qquad c \leq x \leq \infty$$

A 'bound vorticity' distribution $\gamma(x,y)$ and a 'trailing vorticity' distribution $\delta(x,y)$ are introduced about mutually perpendicular directions as shown in Fig. 1. These vorticity distributions over the wing are related by the equation of continuity of vorticity

$$\frac{\partial \gamma(x,y)}{\partial y} = -\frac{\partial \delta(x,y)}{\partial x} \qquad \cdots (1)$$

To comply with the conditions of leading edge separation the upwash just off the leading edge must be finite. It should be noted that this condition does not imply zero loading at the leading edge although it does preclude an infinite loading there.

Following/

Following the observations of Brown and Michael[2] finite upwash velocities off the leading edge are ensured if the vorticity parallel to the leading edge tends to zero as the square root of the distance from the leading edge, the vorticity normal to the leading edge at the leading edge remains finite and represents the feeding vorticity connected through a 'cut' to the main separated 'concentrated' vortices. In general, the vorticity on the wing S_W can be written

$$\gamma(x,y) = \gamma_1(x,y) + \gamma_g(x,y) \qquad \cdots (2)$$

$$\delta(x,y) = \delta_1(x,y) + \delta_g(x,y) \qquad \cdots (3)$$

where the functions $\gamma_1(x,y)$ and $\delta_1(x,y)$ both tend to zero as the square root of the distance from the leading edge; at the leading edge the functions $\gamma_g(x,y)$ and $\delta_g(x,y)$ are both finite and their resultant vorticity is normal to the leading edge. The 'vorticity' distribution representing $\gamma_g(x,y)$ and $\delta_g(x,y)$ in the present case of a delta wing is assumed to comprise lines of constant vorticity on circular arcs with the apex as their centre. The resultant vorticity at the leading edge is therefore at right-angles to it, as indicated in Fig. 2. The expressions for $\gamma_g(x,y)$ and $\delta_g(x,y)$ can be written.

$$\gamma_g(x,y) = \cos\theta_L \cdot \left(\frac{d\Gamma_W}{dx}\right)_{x=\left(\frac{x^2+y^2}{1+k^2}\right)^{1/2}} = \frac{x}{(x^2+y^2)^{1/2}} \cdot \left(\frac{d\Gamma_W}{dx}\right)_{x=\left(\frac{x^2+y^2}{1+k^2}\right)^{1/2}} \qquad \cdots (4)$$

$$\delta_g(x,y) = -\sin\theta_L \cdot \left(\frac{d\Gamma_W}{dx}\right)_{x=\left(\frac{x^2+y^2}{1+k^2}\right)^{1/2}} = \frac{-y}{(x^2+y^2)^{1/2}} \cdot \left(\frac{d\Gamma_W}{dx}\right)_{x=\left(\frac{x^2+y^2}{1+k^2}\right)^{1/2}} . \qquad \cdots (5)$$

Next the conditions at the trailing edge are discussed. Because of the outward deflection of the streamlines and vortex lines at the trailing edge both $\gamma(c,y)$ and $\delta(c,y)$ will exist. Straight filaments of vorticity leave the trailing edge at an angle $\beta(y)$ in the present model and continue downstream until reaching the edge of S_T where they are immediately convected into the main vortex via the 'cut' to increase the vortex strength $\Gamma_T(x)$. The angle $\beta(y)$ is given by

$$\tan\beta(y) = \frac{v_\Gamma(c,y,o)}{V\cos\alpha + u_\Gamma(c,y,o)} \qquad \cdots (6)$$

where $v_\Gamma(c,y,o)$ and $u_\Gamma(c,y,o)$ are the velocity components induced at the trailing edge by separated line vortices. Since the zero load condition at the trailing edge is satisfied if

$$\gamma(c,y).(V\cos\alpha + u_\Gamma(c,y,o)) - \delta(c,y).\, v_\Gamma(c,y,o) = 0 \qquad \cdots (7)$$

then from equations (6) and (7)

$\gamma(c,y)/$

$$\frac{\gamma(c,y)}{\delta(c,y)} = \frac{v_T(c,y,o)}{V\cos\alpha + u_T(c,y,o)} = \tan\beta(y) \quad . \qquad \cdots (8)$$

A relationship between the vorticity shed at the trailing edge and the strength of 'trailing' vortices $\Gamma_T(x)$ can be deduced. By reference to Fig. 3, if A is a point on the trailing edge and D is a point on the side edge of S_T such that AD is at an angle $\beta(y)$ to the $\bar{x}$-axis, then the circulation about the strip along AD of width δn is equal to $\delta(c,y).dy$ $(= \gamma(c,y).dx)$. The addition to the trailing vortex $\Gamma_T(x)$ from the wake can therefore be written as

$$\left(\frac{d\Gamma_T}{dx}\right)_{x = [(s-y)\cot\beta(y)+c]} = \gamma(c,y) \qquad \cdots (9)$$

or

$$\Gamma_T(x = [(s-y)\cot\beta(y) + c]) = \int_y^s \delta(c,y')\, dy' \quad . \qquad \cdots (10)$$

Thus the vorticity distribution in the wake S_T together with the vortex strength Γ_T can be expressed in terms of the wing vorticity distribution over S_W and the trailing edge shedding angle $\beta(y)$.

The problem reduces to the determination of the following unknowns:

(i) the strength of vorticity components $\gamma_1(x,y)$ and $\delta_1(x,y)$ on the wing S_W ,

(ii) the strength of the main vortices $\Gamma_W(x)$ over the wing S_W ,

(iii) $\beta(y)$,

(iv) the position of the main vortices over S_W and S_T .

The boundary conditions to be applied for the calculation of these unknowns are:

(i) the flow is tangential over the surface of the wing S_W ,

(ii) zero load at the trailing edge,

(iii) zero force on the vortex-cut arrangement over both the wing S_W and the trailing sheet S_T ; it is assumed in this paper that the force components in y- and z- directions are the important ones, the x-component force is not considered.

II.2 Calculation of induced velocities

II.2.1 Velocities induced by the wing vorticity distributions $\gamma(x,y)$ and $\delta(x,y)$

The non-dimensional induced velocities $\bar{u}_W(\bar{x}_1,\bar{y}_1,\bar{z}_1)$, $\bar{v}_W(\bar{x}_1,\bar{y}_1,\bar{z}_1)$ and $w_W(\bar{x}_1,\bar{y}_1,\bar{z}_1)$ due to the vorticity distributions

$\bar{v}$/

$\bar{\gamma}(\bar{x},\bar{y})$ and $\bar{\delta}(\bar{x},\bar{y})$ distributed over S_W, in terms of the non-dimensional parameters defined in the Notation, are

$$\bar{u}_W(\bar{x}_1,\bar{y}_1,\bar{z}_1) = \frac{1}{4\pi}\iint_{S_W} \bar{\gamma}(\bar{x},\bar{y}) \frac{\bar{z}_1}{[(\bar{x}-\bar{x}_1)^2+(\bar{y}-\bar{y}_1)^2+\bar{z}_1^2]^{3/2}}\, d\bar{x}\, d\bar{y} \quad \cdots (11)$$

$$\bar{v}_W(\bar{x}_1,\bar{y}_1,\bar{z}_1) = -\frac{1}{4\pi}\iint_{S_W} \bar{\delta}(\bar{x},\bar{y}) \frac{\bar{z}_1}{[(\bar{x}-\bar{x}_1)^2+(\bar{y}-\bar{y}_1)^2+\bar{z}_1^2]^{3/2}}\, d\bar{x}\, d\bar{y} \quad \cdots (12)$$

$$\bar{w}_W(\bar{x}_1,\bar{x}_1,\bar{z}_1) = \frac{1}{4\pi}\iint_{S_W} \frac{(\bar{x}-\bar{x}_1)\,\bar{\gamma}(\bar{x},\bar{y}) - (\bar{y}-\bar{y}\ )\,\bar{\delta}(\bar{x},\bar{y})}{[(\bar{x}-\bar{x}_1)^2+(\bar{y}-\bar{y}_1)^2+\bar{z}_1^2]^{3/2}}\, d\bar{x}\, d\bar{y}\,. \quad \cdots (13)$$

The subscript W on the velocity components indicates that the velocities are induced by the wing vorticity. As far as satisfying this condition of tangency of flow on S_W to a first order, only $\bar{w}_W(\bar{x}_1,\bar{y}_1,+0)$ from equation (13) is required, this is the classical linearised downwash integral where the integrand possesses the usual singular behaviour as $\bar{z}_1 \to 0$. The other velocity components $\bar{u}_W(\bar{x}_1,\bar{y}_1,\bar{z}_1)$ (equation (11)) and $\bar{v}_W(\bar{x}_1,\bar{y}_1,\bar{z}_1)$ (equation 12)) will be required in the calculation of the velocity fields around the leading edge vortices.

II.2.2 <u>Velocities induced by the vorticity on S_T</u>

As described in Section I, the trailing vortex sheet S_T consists of straight filaments of constant vorticity which leave the trailing edge at an angle $\beta(y)$. First the downwash due to the filament AD (shown on Fig. 3) is derived. Taking x_ℓ, y_ℓ as a general point on the line AD the equation of AD may be written in non-dimensional terms,

$$\bar{x}_\ell = (\bar{y}_\ell - \bar{y}) \cot\beta(\bar{y}) + 1 \quad \cdots (14)$$

Thus the angle $\beta(\bar{y})$ is given by

$$\tan\beta(\bar{y}) = \frac{d\bar{y}_\ell}{d\bar{x}_\ell} = \frac{\bar{\gamma}(1,\bar{y})}{\bar{\delta}(1,\bar{y})} \quad \cdots (15)$$

using equation (8).

First the important upwash velocity in the $\bar{z}$-direction is considered. The induced upwash due to AD at a general point $P(\bar{x}_1,\bar{y}_1,\bar{z}_1)$, denoted by $\Delta\bar{w}_{AD}$, is

$\Delta\bar{w}_{AD}$ /

$$\Delta\bar{w}_{AD}(\bar{x}_1,\bar{y}_1,\bar{z}_1) = \bar{\delta}(1,\bar{y}).d\bar{y}.\frac{1}{4\pi}\int_{\bar{y}_\ell=\bar{y}}^{\bar{y}_\ell=k} \frac{(\bar{x}_\ell - \bar{x}_1)d\bar{y}_\ell - (\bar{y}_\ell - \bar{y}_1)\dfrac{d\bar{x}_\ell}{d\bar{y}_\ell}d\bar{y}_\ell}{[(\bar{x}_\ell - \bar{x}_1)^2 + (\bar{y}_\ell - \bar{y}_1)^2 + z_1^2)]^{3/2}} \qquad \ldots (16)$$

Integration of equation (16) between the limits $0,k$ yields the effect of the right-hand side of the trailing sheet S_T in inducing upwash at a point $P(\bar{x}_1,\bar{y}_1,\bar{z}_1)$; writing this term as $\bar{w}_{T_R}$ then

$$\bar{w}_{T_R}(\bar{x}_1,\bar{y}_1,\bar{z}_1) = \frac{1}{4\pi}\int_0^k \bar{\delta}(1,\bar{y}).\{(1 - \bar{x}_1) - (\bar{y} - \bar{y}_1)\cot\beta(\bar{y})\}[I(\bar{y})]\,d\bar{y} \qquad \ldots (17)$$

where

$$I(\bar{y}) = \int_{\bar{y}}^k \frac{d\bar{y}_\ell}{[\{\bar{y}_\ell - \bar{y})\cot\beta(\bar{y}) + (1 - \bar{x}_1)\}^2 + (\bar{y}_\ell - \bar{y}_1)^2 + z_1^2]^{3/2}} \qquad \ldots (18)$$

after substituting for $\bar{x}_\ell$ and $\dfrac{d\bar{y}_\ell}{d\bar{x}_\ell}$ from equations (14) and (15).
The analytic reduction of $I(\bar{y})$ is dealt with in Appendix II. The corresponding expression for the induced upwash effect due to the left-hand side wake $\bar{w}_{T_L}$ is simply obtained by changing the sign of $\bar{y}_1$ in the expression for $\bar{w}_{T_R}$, thus

$$\bar{w}_{T_L}(\bar{x}_1,\bar{y}_1,\bar{z}_1) = \bar{w}_{T_R}(\bar{x}_1,-\bar{y}_1,\bar{z}_1) \ . \qquad \ldots (19)$$

The total upwash effect due to trailing vortex sheet S_T is therefore

$$\bar{w}_T(\bar{x}_1,\bar{y}_1,\bar{z}_1) = \bar{w}_{T_R}(\bar{x}_1,\bar{y}_1,\bar{z}_1) + \bar{w}_{T_L}(\bar{x}_1,\bar{y}_1,\bar{z}_1) \qquad \ldots (20)$$

The induced velocities $\bar{u}_T$ and $\bar{w}_T$ due to the wake can be derived in a similar manner to that outlined for $\bar{w}_T$ above; it is found that

$$\bar{u}_{T_R}(\bar{x}_1,\bar{y}_1,\bar{z}_1) = \bar{u}_{T_L}(\bar{x}_1,-\bar{y}_1,\bar{z}_1) = \frac{\bar{z}_1}{4\pi}\int_0^k \bar{\delta}(1,\bar{y}).\ [I(\bar{y})]\,d\bar{y} \qquad \ldots (21)$$

$$\bar{v}_{T_R}(\bar{x}_1,\bar{y}_1,\bar{z}_1) = \bar{v}_{T_L}(\bar{x}_1,-\bar{y}_1,\bar{z}_1) = \frac{\bar{z}_1}{4\pi}\int_0^k \bar{\delta}(1,\bar{y}).\cot\beta(\bar{y}).[I(\bar{y})]\,d\bar{y} \qquad \ldots (22)$$

II.2.3 Velocities induced by the discrete main line vortices

Expressions for the velocities induced at a general point by the right-hand vortex are derived first. The three induced velocity components $\bar{u}_{\Gamma_R}$, $\bar{v}_{\Gamma_R}$ and $\bar{w}_{\Gamma_R}$ due to right-hand vortex of non-dimensional strength $\bar{\Gamma}(\bar{x})$ can be written in the concise form

$\bar{u}_{\Gamma_R}$/

$$\bar{u}_{\Gamma_R}(\bar{x}_1,\bar{y}_1,\bar{z}_1) = \int_0^\infty \bar{\Gamma}(\bar{x}).f_u(\bar{x},\bar{x}_1,\bar{y}_1,\bar{z}_1)\ d\bar{x} \qquad \cdots (23)$$

$$\bar{v}_{\Gamma_R}(\bar{x}_1,\bar{y}_1,\bar{z}_1) = \int_0^\infty \bar{\Gamma}(\bar{x}).f_v(\bar{x},\bar{x}_1,\bar{y}_1,\bar{z}_1)\ d\bar{x} \qquad \cdots (24)$$

$$\bar{w}_{\Gamma_R}(\bar{x}_1,\bar{y}_1,\bar{z}_1) = \int_0^\infty \bar{\Gamma}(\bar{x}).f_w(\bar{x},\bar{x}_1,\bar{y}_1,\bar{z}_1)\ d\bar{x} \qquad \cdots (25)$$

where

$$f_u(\bar{x},\bar{x}_1,\bar{y}_1,\bar{z}_1) = \frac{1}{4\pi} \cdot \frac{(\bar{y}_v(\bar{x}) - \bar{y}_1)\dfrac{d\bar{z}_v(\bar{x})}{dx} - (\bar{z}_v(\bar{x}) - \bar{z}_1)\dfrac{d\bar{y}_v(\bar{x})}{d\bar{x}}}{[(\bar{x} - \bar{x}_1)^2 + (\bar{y}_v(\bar{x}) - \bar{y}_1)^2 + (\bar{z}_v(\bar{x}) - \bar{z}_1)^2]^{3/2}} \qquad \cdots (26)$$

$$f_v(\bar{x},\bar{x}_1,\bar{y}_1,\bar{z}_1) = \frac{1}{4\pi} \cdot \frac{(\bar{z}_v(\bar{x}) - \bar{z}_1) - (\bar{x} - \bar{x}_1)\dfrac{d\bar{z}_v(\bar{x})}{d\bar{x}}}{[(\bar{x} - \bar{x}_1)^2 + (\bar{y}_v(\bar{x}) - \bar{y}_1)^2 + (\bar{z}_v(x) - \bar{z}_1)^2]^{3/2}} \qquad \cdots (27)$$

$$f_w(\bar{x},\bar{x}_1,\bar{y}_1,\bar{z}_1) = \frac{1}{4\pi} \cdot \frac{(\bar{x} - \bar{x}_1)\dfrac{d\bar{y}_v(\bar{x})}{d\bar{x}} - (\bar{y}_v(\bar{x}) - \bar{y}_1)}{[(\bar{x} - \bar{x}_1)^2 + (\bar{y}_v(\bar{x}) - \bar{y}_1)^2 + (\bar{z}_v(\bar{x}) - \bar{z}_1)^2]^{3/2}} \qquad \cdots (28)$$

Since $\bar{\Gamma}(\bar{x})$ has been separated into the form

$$\begin{aligned}\bar{\Gamma}(\bar{x}) &= \bar{\Gamma}_W(\bar{x}) && \text{for} \quad 0 \leqslant \bar{x} \leqslant 1 \quad \text{(i.e. over the wing)} \\ &= \bar{\Gamma}_W(1) + \bar{\Gamma}_T(\bar{x}) && \text{for} \quad 1 < \bar{x} \leqslant \infty \quad \text{(i.e. in the wake)}\end{aligned} \qquad \cdots (29)$$

the induced velocities due to $\bar{\Gamma}_W(\bar{x})$ and $\bar{\Gamma}_T(\bar{x})$ can also be separated. Thus the three induced velocities can be written

$$\bar{u}_{\Gamma_R}(\bar{x}_1,\bar{y}_1,\bar{z}_1) = \bar{u}_{\Gamma_{W_R}}(\bar{x}_1,\bar{y}_1,\bar{z}_1) + \bar{u}_{\Gamma_{T_R}}(\bar{x}_1,\bar{y}_1,\bar{z}_1)$$

$$\bar{v}_{\Gamma_R}(\bar{x}_1,\bar{y}_1,\bar{z}_1) = \bar{v}_{\Gamma_{W_R}}(\bar{x}_1,\bar{y}_1,\bar{z}_1) + \bar{v}_{\Gamma_{T_R}}(\bar{x}_1,\bar{y}_1,\bar{z}_1)$$

$$\bar{w}_{\Gamma_R}(\bar{x}_1,\bar{y}_1,\bar{z}_1) = \bar{w}_{\Gamma_{W_R}}(\bar{x}_1,\bar{y}_1,\bar{z}_1) + \bar{w}_{\Gamma_{T_R}}(\bar{x}_1,\bar{y}_1,\bar{z}_1)$$

where

$\bar{u}_{\Gamma_{W_R}}$/

$$\bar{u}_{\Gamma_{W_R}}(\bar{x}_1,\bar{y}_1,\bar{z}_1) = \int_0^1 \bar{\Gamma}_W(\bar{x}).f_u(\bar{x},\bar{x}_1,\bar{y}_1,\bar{z}_1)\ d\bar{x} + \bar{\Gamma}_W(1)\int_1^\infty f_u(\bar{x},\bar{x}_1,\bar{y}_1,\bar{z}_1)\ d\bar{x} \quad \cdots (30)$$

$$\bar{v}_{\Gamma_{W_R}}(\bar{x}_1,\bar{y}_1,\bar{z}_1) = \int^1 \bar{\Gamma}_W(\bar{x}).f_v(\bar{x},\bar{x}_1,\bar{y}_1,\bar{z}_1)\ d\bar{x} + \bar{\Gamma}_W(1)\int_1^\infty f_v(\bar{x},\bar{x}_1,\bar{y}_1,\bar{z}_1)\ d\bar{x} \quad \cdots (31)$$

$$\bar{w}_{\Gamma_{W_R}}(\bar{x}_1,\bar{y}_1,\bar{z}_1) = \int_0^1 \bar{\Gamma}_W(\bar{x}) f_w(\bar{x},\bar{x}_1,\bar{y}_1,\bar{z}_1)\ d\bar{x} + \bar{\Gamma}_W(1)\int_1^\infty f_w(\bar{x},\bar{x}_1,\bar{y}_1,\bar{z}_1)\ d\bar{x} \quad \cdots (32)$$

$$\begin{aligned}\bar{u}_{\Gamma_{T_R}}(\bar{x}_1,\bar{y}_1,\bar{z}_1) &= \int_1^\infty \bar{\Gamma}_T(\bar{x}).f_u(\bar{x},\bar{x}_1,\bar{y}_1,\bar{z}_1)\ d\bar{x} \\ &= \int_k^\rho \left[\int_{\bar{y}}^k \bar{\delta}(1,\bar{y}')\ d\bar{y}'\right]\left\{f_u([(k-\bar{y}).\cot\beta(\bar{y})+1],\bar{x}_1,\bar{y}_1,\bar{z}_1)\right\} \\ &\times\left\{-\cot\beta(\bar{y}) - (k-\bar{y})\operatorname{cosec}^2\beta(\bar{y})\frac{\partial\beta(\bar{y})}{d\bar{y}}\right\} d\bar{y}\end{aligned} \quad \cdots (33)$$

$$\begin{aligned}\bar{v}_{\Gamma_{T_R}}(\bar{x}_1,\bar{y}_1,\bar{z}_1) &= \int_1^\infty \bar{\Gamma}_T(\bar{x}).f_v(\bar{x},\bar{x}_1,\bar{y}_1,\bar{z}_1)\ d\bar{x} \\ &= \int_k^o \left[\int_y^k \delta(1,\bar{y}')\ dy'\right]\left\{f_v([(k-\bar{y})\cot\beta(\bar{y})+1],x_1,y_1,z_1)\right\} \\ &\times\left\{-\cot\beta(\bar{y}) - (k-\bar{y})\operatorname{cosec}^2\beta(\bar{y})\frac{\partial\beta(\bar{y})}{\partial y}\right\}.d\bar{y}\end{aligned} \quad \cdots (34)$$

$$\begin{aligned}\bar{w}_{\Gamma_{T_R}}(\bar{x}_1,\bar{y}_1,\bar{z}_1) &= \int_1^\infty \bar{\Gamma}_T(\bar{x}).f_w(\bar{x},\bar{x}_1,\bar{y}_1,\bar{z}_1)\ d\bar{x} \\ &= \int_k^o \left[\int_y^k \bar{\delta}(1,y')\ d\bar{y}'\right]\left\{f_w([(k-\bar{y})\cot\beta(\bar{y})+1],\bar{x}_1,\bar{y}_1,\bar{z}_1)\right\} \\ &\times\left\{-\cot\beta(\bar{y}) - (k-\bar{y})\operatorname{cosec}^2\beta(\bar{y})\frac{\partial\beta(\bar{y})}{\partial\bar{y}}\right\} d\bar{y}\end{aligned} \quad \cdots (35)$$

The/

The last three equations (33), (34) and (35) have been transformed into spanwise integrals since $\bar{\Gamma}_T(\bar{x})$ is known only as a function of $\bar{y}$ by the statement leading to equations (10) and (14), the transformation used is

$$\bar{x} = (k - \bar{y}) \cot \beta(\bar{y}) + 1 \cdot$$

Corresponding expressions for the induced velocities $\bar{u}_{\Gamma_{W_L}}(\bar{x}_1,\bar{y}_1,\bar{z}_1)$, $w_{\Gamma_{W_L}}(\bar{x}_1,\bar{y}_1,\bar{z}_1)$, $\bar{u}_{\Gamma_{T_L}}(\bar{x}_1,\bar{y}_1,\bar{z}_1)$ and $\bar{w}_{\Gamma_{T_L}}(x_1,y_1,z_1)$ due to the left-hand vortex may be derived by changing the sign of $\bar{y}_1$ in equations (30), (32), (33) and (35), while $\bar{v}_{\Gamma_{W_L}}(x_1,y_1,z_1)$ and $\bar{v}_{\Gamma_{T_L}}(\bar{x}_1,\bar{y}_1,\bar{z}_1)$ are given by changing the sign of $\bar{y}_1$ and the overall signs of equations (31) and (34).

II.3 Application of the boundary conditions

The boundary conditions representing the tangency of flow over wing and zero force on the vortex-cut arrangement are now formulated. It is assumed that the condition of zero pressure loading on the trailing vortex sheet need not be considered further since the wake model has been designed to meet this requirement.

For a flat wing at incidence α the condition of tangency of flow over the wing surface in non-dimensional terms is

$$\bar{w}(\bar{x}_1,\bar{y}_1,o) = - \sin \alpha \cdot \qquad \ldots (36)$$

The induced upwash velocity $\bar{w}(x_1,y_1,o)$ includes the contributions from the vorticity on the wing surface S_W , the vorticity on the trailing vortex sheet S_T and the main concentrated vortices above both S_W and S_T , therefore

$$\bar{w}(\bar{x}_1,\bar{y}_1,o) = \bar{w}_W(\bar{x}_1,\bar{y}_1,o) + \bar{w}_T(\bar{x}_1,\bar{y}_1,o) + \bar{w}_{\Gamma_W}(\bar{x}_1,\bar{y}_1,o) + \bar{w}_{\Gamma_T}(\bar{x}_1,\bar{y}_1,o) \qquad \ldots (37)$$

where all of these contributions have been defined in Section II.2.

Zero loading of the vortex-cut combination is satisfied on the starboard system only, then by symmetry the port system will also be satisfied. Only the force components in the $\bar{y}$- and $\bar{z}$- directions are considered since it is thought that these flow forces are the significant ones, effectively the force components normal to the vortex should have been used but the extra computational effort is probably not justified at this stage.

The force on $\bar{\Gamma}(\bar{x})$ at $(\bar{x},\bar{y}_v(\bar{x}),\bar{z}_v(\bar{x}))$ is

$\rho V^2 c$ ./

$$\rho V^2 c \,.\, \bar{\Gamma}(\bar{x}) \,.\, d\bar{x} \,.\left[\frac{d\bar{y}_v(\bar{x})}{d\bar{x}} - \bar{v}_1(\bar{x},\bar{y}_v(\bar{x}),\bar{z}_v(x)) \right]$$

in the $\bar{z}$-direction ... (38)

and $$-\rho V^2 c \,.\, \bar{\Gamma}(\bar{x}) \,.\, d\bar{x} \,.\left[\frac{d\bar{z}_v(\bar{x})}{d\bar{z}} - \bar{w}_1(\bar{x},\bar{y}_v(\bar{x}),\bar{z}_v(\bar{x})) \right] \qquad \text{... (39)}$$

in the $\bar{y}$-direction. These relationships are to be applied over both S_W and S_T .

The first terms in equations (38) and (39) represent the force on the vortex due to the free stream V . The second terms represent the force on the vortex due to the perturbation velocities $\bar{v}_1(\bar{x},\bar{y}_v(\bar{x}),\bar{z}_v(\bar{x}))$ and $\bar{w}_1(\bar{x},\bar{y}_v(\bar{x}),\bar{z}_v(\bar{x}))$ induced at the point $(\bar{x},\bar{y}_v(\bar{x}),\bar{z}_v(\bar{x}))$ on the starboard main vortex by the whole system of vorticity but excluding the starboard main vortex itself. Theoretically since each main vortex is curved it induces an infinite velocity on itself; this infinite velocity is not included in the subsequent analysis. Intuitively it would be expected that these self-induced velocities would be small compared with all the other induced velocities but there appears to be no valid reason for ignoring this behaviour, in any case the authors were not sure how this effect should be incorporated into the analysis in a simple way. The breakdown of the induced velocities from the various sources can be written

$$\begin{aligned} \bar{v}_1(\bar{x},\bar{y}_v(\bar{x}),\bar{z}_v(\bar{x})) = \; & \bar{v}_W(\bar{x},\bar{y}_v(\bar{x}),\bar{z}_v(\bar{x})) \\ & + \bar{v}_T(\bar{x},\bar{y}_v(\bar{x}),\bar{z}_v(\bar{x})) \\ & + \bar{v}_{\Gamma_{W_L}}(\bar{x},\bar{y}_v(\bar{x}) , \bar{z}_v(\bar{x})) \\ & + \bar{v}_{\Gamma_{T_L}}(\bar{x},\bar{y}_v(\bar{x}),\bar{z}_v(\bar{x})) \end{aligned} \qquad \text{... (40)}$$

$$\begin{aligned} \bar{w}_1(\bar{x},\bar{y}_v(\bar{x}),\bar{z}_v(\bar{x})) = \; & \bar{w}_W(\bar{x},\bar{y}_v(\bar{x}),\bar{z}_v(\bar{x})) \\ & + \bar{w}_T(\bar{x},\bar{y}_v(\bar{x}),\bar{z}_v(\bar{x})) \\ & + \bar{w}_{\Gamma_{W_L}}(\bar{x},\bar{y}_v(\bar{x}),\bar{z}_v(\bar{x})) \\ & + \bar{w}_{\Gamma_{T_L}}(\bar{x},\bar{y}_v(\bar{x}),\bar{z}_v(\bar{x})) \end{aligned} \qquad \text{... (41)}$$

where the various terms are given in Section II.2.

The force components on the cut arise mainly from the free stream V because the streamwise perturbation velocities are small in comparison with V ; these force components are therefore

$\rho V^2 c$./

$$\rho V^2 c \,.\, \frac{d\bar{\Gamma}(\bar{x})}{d\bar{x}} \left(\bar{y}_v(\bar{x}) - k\bar{x}\right) d\bar{x} \qquad \text{in the } \bar{z}\text{-direction} \qquad \ldots (42)$$

and
$$-\rho V^2 c \,.\, \frac{d\bar{\Gamma}(\bar{x})}{d\bar{x}} \cdot \bar{z}_v(\bar{x}) \qquad \text{in the } \bar{y}\text{-direction} \qquad \ldots (43)$$

Thus the total force components on the vortex-cut arrangement in $\bar{y}$- and $\bar{z}$- directions, combining equations (38), (39), (42), (43) are

$$F_y(\bar{x}) = -2\bar{\Gamma}(x)\left[\frac{d\bar{z}_v(\bar{x})}{d\bar{x}} + \frac{1}{\bar{\Gamma}(\bar{x})} \cdot \frac{d\bar{\Gamma}(\bar{x})}{d\bar{x}} \cdot \bar{z}_v(\bar{x}) - \bar{w}_1(\bar{x},\bar{y}_v(\bar{x}),\bar{z}_v(\bar{x}))\right] \qquad \ldots (44)$$

$$F_z(\bar{x}) = +2\bar{\Gamma}(x)\left[\frac{d\bar{y}_v(\bar{x})}{d\bar{x}} + \frac{1}{\bar{\Gamma}(\bar{x})} \cdot \frac{d\bar{\Gamma}(\bar{x})}{d\bar{x}} \cdot (\bar{y}_v(\bar{x}) - kx) - \bar{v}_1(\bar{x},\bar{y}_v(\bar{x}),\bar{z}_v(\bar{x}))\right]. \qquad \ldots (45)$$

In accordance with the boundary conditions these two forces $F_y(\bar{x})$ and $F_z(\bar{x})$ are to be made zero. As stated earlier, the numerical procedure is to assume an 'initial' vortex position and to apply the boundary conditions of tangency of flow and zero load at the trailing edge. And then the velocities $\bar{v}_1(\bar{x},\bar{y}_v(\bar{x}),\bar{z}_v(\bar{x}))$ and $\bar{w}_1(\bar{x},\bar{y}_v(\bar{x}),\bar{z}_v(\bar{x}))$ can be calculated at the 'initial' vortex position so equations (44) and (45) can be used to estimate a 'new' vortex position. It has been the experience of Smith[5] and the authors that the forces $F_y(\bar{x})$ and $F_z(\bar{x})$ are extremely sensitive to vortex position. To derive a new vortex position by simply equating the forces to zero can lead to large movements from the initial positions; in fact the authors found this procedure divergent.

To avoid divergence, the movement of the vortex is restricted. A new vortex position is calculated only if the force on it exceeds a pre-specified 'tolerance' and then the vortex is moved a small amount in the direction of resultant force (components F_y and F_z) to a 'new' vortex position.

The resultant force vector $F(\bar{x})$ at the starboard vortex is given by

$$F(\bar{x}) = \left(F_y^2(\bar{x}) + F_z^2(\bar{x})\right)^{1/2} \qquad \ldots (46)$$

and its angle of inclination to xy- plane is given by

$$\tan^{-1}\left(\frac{F_z(\bar{x})}{F_y(\bar{x})}\right). \qquad \ldots (47)$$

The 'corrections' to the slopes of the vortex geometry are then given by

$$\frac{d}{dx}\left(\Delta\bar{z}_v(\bar{x})\right) = d_{tol} \cdot \frac{F_y(\bar{x})}{F(\bar{x})} \qquad (\text{if } F(\bar{x}) \geqslant F_{tol}) \qquad \ldots (48)$$

$$\frac{d}{dx}\left(\Delta\bar{y}_v(\bar{x})\right) = -d_{tol} \cdot \frac{F_z(\bar{x})}{F(\bar{x})} \qquad (\text{if } F(\bar{x}) \geqslant F_{tol}) \qquad \ldots (49)$$

where/

where d_{tol} is a small specified 'tolerance' in the slopes of the vortex geometry and F_{tol} is a small tolerance for the force.

The actual 'corrections' to the vortex geometry can then be written

$$\Delta\bar{z}_v(\bar{x}) = \int_0^{\bar{x}} \frac{d}{dx}\,(\Delta\bar{z}_v(\bar{x}'))\,d\bar{x}' \qquad \ldots (50)$$

$$\Delta\bar{y}_v(\bar{x}) = \int_0^{\bar{x}} \frac{d}{dx}\,(\Delta\bar{y}_v(\bar{x}'))\,d\bar{x}' \qquad \ldots (51)$$

which leads to the 'new' position of the vortex

$$\underset{\text{new}}{\bar{y}_v(\bar{x})} = \underset{\text{initial}}{\bar{y}_v(\bar{x})} + \Delta\bar{y}_v(\bar{x}) \qquad (0 \leqslant \bar{x} \leqslant \infty) \qquad \ldots (52)$$

$$\underset{\text{new}}{\bar{z}_v(\bar{x})} = \underset{\text{initial}}{\bar{z}_v(\bar{x})} + \Delta\bar{z}_v(\bar{x}) \qquad (0 \leqslant \bar{x} \leqslant \infty) \qquad \ldots (53)$$

II.4 Numerical method

The unknowns in the present problem are:

(i) the related vorticity distributions $\bar{\gamma}(\bar{x},\bar{y})$ and $\bar{\delta}(\bar{x},\bar{y})$ over the wing S_W

(ii) the main vortex strength $\bar{\Gamma}_W(\bar{x})$ over the wing S_W

(iii) the main vortex positions $\bar{y}_v(\bar{x})$ and $\bar{z}_v(\bar{x})$ over both the wing S_W and the trailing vortex sheet S_T

The vorticity in the trailing vortex sheet S_T and the partial contribution to the wake vortex $\bar{\Gamma}_T(\bar{x})$ have been expressed in terms of the vorticity distribution over the wing from the condition of zero load at the trailing edge as indicated in Section II.1.

As discussed in Section II.1 (equations (2)-(5)) the vorticity distributions $\bar{\delta}(\bar{x},\bar{y})$ and $\bar{\gamma}(\bar{x},\bar{y})$ over the wing S_W, are divided into two parts

$$\bar{\delta}(\bar{x},\bar{y}) = \bar{\delta}_1(\bar{x},\bar{y}) + \bar{\delta}_g(\bar{x},\bar{y}) \qquad \ldots (54)$$

$$\bar{\gamma}(\bar{x},\bar{y}) = \bar{\gamma}_1(\bar{x},\bar{y}) + \bar{\gamma}_g(\bar{x},\bar{y}) \qquad \ldots (55)$$

where $\bar{\delta}_1(\bar{x},\bar{y})$ and $\bar{\gamma}_1(\bar{x},\bar{y})$ are continuous functions which tend to zero at the leading edge with the square root of the distance from the leading edge while $\bar{\delta}_g(\bar{x},\bar{y})$ and $\bar{\gamma}_g(\bar{x},\bar{y})$ are related to the strength of the cut $\dfrac{d\bar{\Gamma}_W(\bar{x})}{d\bar{x}}$. In particular, equations (4) and (5) can be written in the non-dimensional form

$\bar{\gamma}_g$/

$$\bar{\gamma}_g(\bar{x},\bar{y}) = \frac{\bar{x}}{(\bar{x}^2+\bar{y}^2)^{1/2}} \cdot \left(\frac{d\Gamma_W(\bar{x})}{d\bar{x}}\right)_{\bar{x}=\left(\frac{\bar{x}^2+\bar{y}^2}{1+k^2}\right)^{1/2}} \qquad \ldots (56)$$

$$\bar{\delta}_g(\bar{x},\bar{y}) = \frac{-\bar{y}}{(\bar{x}^2+\bar{y}^2)^{1/2}} \cdot \left(\frac{d\bar{\Gamma}_W(\bar{x})}{d\bar{x}}\right)_{\bar{x}=\left(\frac{\bar{x}^2+\bar{y}^2}{1+k^2}\right)^{1/2}} . \qquad \ldots (57)$$

II.4.1 <u>Series expansions</u>

A series expansion for wing trailing vorticity $\bar{\delta}_1(\bar{x},\bar{y})$ is taken to be

$$\bar{\delta}_1(\bar{x},\bar{y}) = \sum_{p=0}^{n} \sum_{q=0}^{m} a_{2p+1,q} \cdot \bar{x}^q \cdot \left(\frac{\bar{y}}{k\bar{x}}\right)\left\{1-\left(\frac{\bar{y}}{k\bar{x}}\right)\right\}^{\frac{2p+1}{2}} \qquad \ldots (58)$$

The conservation of vorticity $\left(\text{i.e. } \frac{\partial\bar{\delta}_1(\bar{x},\bar{y})}{\partial\bar{x}} = -\frac{\partial\bar{\gamma}_1(\bar{x},\bar{y})}{\partial\bar{y}}\right)$ leads to the related expansion for $\bar{\gamma}_1(\bar{x},\bar{y})$ namely

$$\bar{\gamma}_1(\bar{x},\bar{y}) = k\sum_{p=0}^{n} \sum_{q=0}^{m} a_{2p+1,q} \cdot \bar{x}^q \cdot \left[\left\{1-\left(\frac{\bar{y}}{k\bar{x}}\right)^2\right\}^{\frac{2p+1}{2}} + \frac{2p-q+2}{2p+3}\left\{1-\left(\frac{y}{kx}\right)^2\right\}^{\frac{2p+3}{2}}\right] . \qquad \ldots (59)$$

It should be noted that the requirement that both $\bar{\delta}_1(\bar{x},\bar{y})$ and $\bar{\gamma}_1(\bar{x},\bar{y})$ tend to zero at the leading edge as the square root of the distance from the leading edge, is built into equations (58) and (59). The expansions in equations (58) and (59) are taken as extensions of slender conical wing distributions omitting the leading edge singularities, thus the usual difficulties in rounding off the wing apex in conventional lifting surface theory do not arise.

A polynomial series expansion is taken for the strength of the leading edge vortex $\bar{\Gamma}_W(\bar{x})$ over the wing S_W in the form

$$\bar{\Gamma}_W(\bar{x}) = \sum_{q=1}^{\ell} g_q \cdot \bar{x}^q . \qquad \ldots (60)$$

The/

The continuation into the wake is discussed later. The vorticity distributions $\bar{\delta}_g(\bar{x},\bar{y})$ and $\bar{\gamma}_g(\bar{x},\bar{y})$ defined in equations (56) and (57) can be expressed in terms of the coefficients g_q introduced in equation (60). The complete expressions for $\bar{\delta}(\bar{x},\bar{y})$ and $\bar{\gamma}(\bar{x},\bar{y})$ become

$$\bar{\delta}(\bar{x},\bar{y}) = \sum_{p=0}^{n} \sum_{q=0}^{m} a_{2p+1,q} \cdot a_\delta(2p+1, q, \bar{x}, \bar{y}) + \sum_{q=1}^{\ell} g_q \cdot g_\delta(q, \bar{x}, \bar{y}) \qquad \cdots (61)$$

$$\bar{\gamma}(\bar{x},\bar{y}) = \sum_{p=0}^{n} \sum_{q=0}^{m} a_{2p+1,q} \cdot a_\gamma(2p+1, q, \bar{x}, \bar{y}) + \sum_{q=1}^{\ell} g_q \cdot g_\gamma(2p+1, q, \bar{x}, \bar{y}) \qquad \cdots (62)$$

where

$$a_\delta(2p+1, q, \bar{x}, \bar{y}) = \bar{x}^q \left(\frac{\bar{y}}{k\bar{x}}\right) \left\{1 - \left(\frac{\bar{y}}{k\bar{x}}\right)^2\right\}^{\frac{2p+1}{2}} \qquad \cdots (63)$$

$$a_\gamma(2p+1, q, x, \bar{y}) = \bar{x}^q . k \left[\left\{1 - \left(\frac{\bar{y}}{k\bar{x}}\right)^2\right\}^{\frac{2p+1}{2}} + \frac{2p - q + 2}{2p + 3} \left\{1 - \left(\frac{\bar{y}}{k\bar{x}}\right)^2\right\}^{\frac{2p+3}{2}} \right] \qquad \cdots (64)$$

$$g_\delta(\bar{q},\bar{x},\bar{y}) = - \frac{\bar{y}}{(\bar{x}^2 + \bar{y}^2)^{1/2}} \cdot q . \left(\frac{\bar{x}^2 + \bar{y}^2}{1 + k^2}\right)^{\frac{q-1}{2}} = \frac{-q}{(1 + k^2)^{\frac{q-1}{2}}} \cdot \bar{y}(\bar{x}^2 + \bar{y}^2)^{\frac{q}{2} - 1} \qquad \cdots (65)$$

$$g_\gamma(\bar{q},\bar{x},\bar{y}) = \frac{\bar{x}}{(\bar{x}^2 + \bar{y}^2)^{1/2}} \cdot q \left(\frac{\bar{x}^2 + \bar{y}^2}{1 + k^2}\right)^{\frac{q-1}{2}} = \frac{q}{(1 + k^2)^{\frac{q-1}{2}}} \bar{x} (\bar{x}^2 + \bar{y}^2)^{\frac{q}{2} - 1} . \qquad \cdots (66)$$

As/

As far as the wake is concerned (i.e. $\bar{x} > 1$) $\bar{\Gamma}_W(1)$ follows from equation (60) and the additional strength $\bar{\Gamma}_T(x)$ can be expressed in terms of the above coefficients using equation (10), by

$$\bar{\Gamma}_T(\bar{x} = [(k - \bar{y}) \cot \beta(\bar{y}) + 1]) = \int_{\bar{y}}^{k} \Big[\sum_{p=0}^{n} \sum_{q=0}^{m} a_{2p+1} \cdot a_\delta(2p+1, q, 1, \bar{y}') + \sum_{q=1}^{\ell} g_q \cdot g_\delta(q, 1, \bar{y}') \Big] d\bar{y}'$$

$$= \sum_{p=0}^{n} \sum_{q=0}^{m} a_{2p+1,q} \cdot \left[+ \frac{k}{2p + 3} \left\{ 1 - \left(\frac{y}{k} \right)^2 \right\}^{\frac{2p+3}{2}} \right] + \sum_{q=1}^{\ell} g_q \cdot \left[- (1 + k^2)^{1/2} + \frac{(1 + y^2)^{\frac{q}{2}}}{(1 + k^2)^{\frac{q-1}{2}}} \right] . \qquad \cdots (67)$$

The strength of the cut in the wake becomes

$$\left(\frac{d\bar{\Gamma}_T(\bar{x})}{d\bar{x}} \right)_{\bar{x} = [(k-\bar{y}) \cot \beta(\bar{y})+1]} = \sum_{p=0}^{n} \sum_{q=0}^{m} a_{2p+1,q} \cdot a_y(2p + 1, q, 1, \bar{y}) . \qquad \cdots (68)$$

II.4.2 <u>Basic equations</u>

Substituting the series expansions for $\bar{\delta}(\bar{x},\bar{y})$ and $\bar{y}(\bar{x},\bar{y})$ into the upwash integral (equation 13)) the induced upwash velocities can be written

$$\bar{w}_W(\bar{x}_1,\bar{y}_1,o) = \sum_{p=0}^{n} \sum_{q=0}^{m} a_{2p+1,q} \cdot aw_W(2p + 1, q, \bar{x}_1,\bar{y}_1) + \sum_{q=1}^{\ell} g_q \cdot gw_W(q,\bar{x}_1,\bar{y}) \qquad \cdots (69)$$

where

$aw_W(2p + 1, q, \bar{x}_1, \bar{y}_1)$

$$= \frac{1}{4\pi} \iint_{\substack{S_W \\ z_1 \to 0}} \frac{(\bar{x} - \bar{x}_1)\, a_y(2p + 1, q, \bar{x}, \bar{y}) - (\bar{y} - \bar{y}_1)\, a_\delta(2p + 1, q, \bar{x}, \bar{y})}{[(\bar{x} - \bar{x}_1)^2 + (\bar{y} - y_1)^2 + z_1^2]^{3/2}} \, d\bar{x}\, d\bar{y} \qquad \cdots (70)$$

and/

and

$$g w_W(q,\bar{x}_1,\bar{y}_1)$$

$$= \frac{1}{4\pi} \iint\limits_{\substack{S_W \\ z_1 \to 0}} \frac{(\bar{x} - \bar{x}_1)\ g_y(q,\bar{x},\bar{y}) - (\bar{y} - \bar{y})\ g_\delta(q,\bar{x},\bar{y})}{[(\bar{x} - \bar{x}_1)^2 + (\bar{y} - \bar{y}_1)^2 + \bar{z}_1]^{3/2}}\ d\bar{x}\ d\bar{y}\ . \qquad \cdots (71)$$

The upwash $\bar{w}_{\Gamma_W}(\bar{x}_1,\bar{y}_1,\bar{z}_1)$ due to the contributions $\bar{\Gamma}_W(\bar{x})$ from the two separated leading edge vortices over S_W together with the contribution $\bar{\Gamma}_W(1)$ aft of the trailing edge is given by substitution of equation (60) into equation (32).

$$\bar{w}_{\Gamma_W}(\bar{x}_1,\bar{y}_1,o) = \sum_{q=1}^{\ell} g_q \cdot g w_{\Gamma_W}(q,\bar{x}_1,\bar{y}_1) \qquad \cdots (72)$$

where

$$g w_{\Gamma_W}(q,\bar{x}_1,\bar{y}_1) = g w_{\Gamma_{W_R}}(q,\bar{x}_1,\bar{y}_1) + g w_{\Gamma_{W_L}}(q,\bar{x}_1,\bar{y}_1)$$

$$= \int_0^1 \bar{x}^q \Big[f_w(\bar{x},\bar{x}_1,\bar{y}_1,o) + f_w(\bar{x},\bar{x}_1,-\bar{y}_1,o) \Big]\, d\bar{x}$$

$$+ \int_1^\infty \Big[f_w(\bar{x},\bar{x}_1,\bar{y}_1,o) + f_w(\bar{x},\bar{x}_1,-\bar{y}_1,o) \Big]\, d\bar{x} \qquad (73)$$

The upwash $\bar{w}_{T_R}(\bar{x}_1,\bar{y}_1,\bar{z}_1)$ due to vorticity on the right half of trailing vortex sheet S_T, defined in equations (17)-(19), becomes, on substitution of equation (58),

$$\bar{w}_{T_R}(\bar{x}_1,\bar{y}_1,o) = \frac{1}{4\pi} \int_{y=0}^{\bar{y}=k} \Big[\sum_{p=0}^{n} \sum_{q=0}^{m} a_{2p+1,q} \cdot a_\delta(2p+1, q, 1, \bar{y})$$

$$+ \sum_{q=1}^{\ell} g_q \cdot g_\delta(q,1,\bar{y}) \Big]$$

$$\cdot \Big[(1 - \bar{x}_1) - (\bar{y} - \bar{y}_1) \cot \beta(\bar{y}) \Big] \Big[I(\bar{y}) \Big]\, d\bar{y} \qquad \cdots (74)$$

The upwash due to the right-hand wake main vortex $\bar{\Gamma}_T(\bar{x})$, defined in equation (35), substituting the expressions in equations (58), (67), becomes

$\bar{w}_{\Gamma_{T_R}}$/

$$\bar{w}_{\Gamma_{T_R}}(\bar{x}_1,\bar{y}_1,o) = \int_{\bar{y}=k}^{\bar{y}=0} \left[\int_{\bar{y}'=\bar{y}}^{\bar{y}'=k} \left\{ \sum_{p=0}^{n} \sum_{q=0}^{m} a_{2p+1,q} \cdot a_\delta(2p+1,q,1,\bar{y}') + \sum_{q=1}^{\ell} g_q \cdot g_\delta(q,1,\bar{y}') \right\} d\bar{y}' \right]$$

$$\cdot \left[f_w(\bar{x} = (k-\bar{y}) \cot\beta(\bar{y}) + 1, \bar{x}_1,\bar{y}_1,o) \right] \cdot \left[-\cot\beta(\bar{y}) - (k-\bar{y}) \operatorname{cosec}^2\beta(\bar{y}) \frac{\partial\beta(\bar{y})}{\partial\bar{y}} \right] \cdot d\bar{y} . \quad \dots (75)$$

And on substitution of equations (63) and (65), equation (75) becomes

$$\bar{w}_{\Gamma_{T_R}}(\bar{x}_1,\bar{y}_1,o) = \int_{o}^{k} \left[\sum_{p=0}^{n} \sum_{q=0}^{m} a_{2p+1,q} \left\{ -\frac{k}{2p+3} \left(1 - \left(\frac{\bar{y}}{k} \right)^2 \right)^{\frac{2p+3}{2}} \right\} + \sum_{q=1}^{\ell} g_q \cdot \left\{ \frac{1}{(1+k^2)^{\frac{q-1}{2}}} \left[(1+k^2)^{\frac{q}{2}} - (1+\bar{y}^2)^{\frac{q}{2}} \right] \right\} \right]$$

$$\cdot \left[f_w(\bar{x} = (k-\bar{y}) \cot\beta(\bar{y}) + 1, \bar{x}_1,\bar{y}_1,o) \right] \cdot \left[-\cot\beta(\bar{y}) - (k-\bar{y}) \operatorname{cosec}^2\beta(\bar{y}) \frac{\partial\beta(\bar{y})}{\partial\bar{y}} \right] \cdot d\bar{y} . \quad \dots (76)$$

These two expressions for $\bar{w}_{T_R}$ and $\bar{w}_{\Gamma_{T_R}}$ together with the symmetrical contribution from the left-hand wake can now be combined to yield an expression of the form

$$\bar{w}_T(\bar{x}_1,\bar{y}_1,o) + \bar{w}_{\Gamma_T}(x_1,y_1,o) = \sum_{p=0}^{n} \sum_{q=0}^{m} a_{2p+1,q} \cdot \left[aw_T(2p+1,q,\bar{x}_1,\bar{y}_1) + aw_{\Gamma_T}(2p+1,q,\bar{x}_1,\bar{y}_1) \right] + \sum_{q=1}^{\ell} g_q \cdot \left[gw_T(q,\bar{x}_1,\bar{y}_1) + gw_{\Gamma_T}(q,\bar{x}_1,\bar{y}_1) \right] \quad \dots (77)$$

where/

where the terms in square brackets involve integration in the $\bar{y}$-direction only and these terms are defined as follows

$$\left[aw_T(2p+1,q,\bar{x}_1,\bar{y}_1) + aw_{\Gamma_T}(2p+1,q,\bar{x}_1,\bar{y}_1)\right]$$

$$= \left[aw_{T_R}(2p+1,q,\bar{x}_1,\bar{y}_1) + aw_{\Gamma_{T_R}}(2p+1,q,\bar{x}_1,\bar{y}_1)\right]$$

$$+ \left[aw_{T_R}(2p+1,q,\bar{x}_1,-\bar{y}_1) + aw_{\Gamma_{T_R}}(2p+1,q,\bar{x}_1,-\bar{y}_1)\right]$$

and

$$\left[gw_T(q,\bar{x}_1,\bar{y}_1) + gw_{\Gamma_T}(q,\bar{x}_1,\bar{y}_1)\right]$$

$$= \left[gw_{T_R}(q,\bar{x}_1,\bar{y}_1) + gw_{\Gamma_{T_R}}(q,\bar{x}_1,\bar{y}_1)\right]$$

$$+ \left[gw_{T_R}(q,x_1,-\bar{y}_1) + gw_{\Gamma_{T_R}}(q,\bar{x}_1,-\bar{y}_1)\right]$$

where

$$\left[aw_{T_R}(2p+1,q,\bar{x}_1,\bar{y}_1) + aw_{\Gamma_{T_R}}(2p+1,q,\bar{x}_1,\bar{y}_1)\right]$$

$$= \left[\int_o^k \left\{ \frac{1}{4\pi}\left(\frac{\bar{y}}{k}\right)\left(1-\left(\frac{\bar{y}}{k}\right)^2\right)^{\frac{2p+1}{2}} \left[(1-\bar{x}_1)-(\bar{y}-\bar{y}_1)\cot\beta(\bar{y})\right]\left[I(\bar{y})\right] \right.\right.$$

$$- \left[\frac{k}{2p+3}\left(1-\left(\frac{y}{k}\right)^2\right)^{\frac{2p+3}{2}}\right]\left[f_w(\bar{x} = (k-\bar{y})\cot\beta(\bar{y})+1,\bar{x}_1,\bar{y}_1,o)\right]$$

$$\left.\left. \cdot \left[-\cot\beta(\bar{y}) - (k-\bar{y})\operatorname{cosec}^2\beta(\bar{y})\frac{\partial\beta}{\partial\bar{y}}\right]\right\} d\bar{y}\right] \qquad \cdots (78)$$

and

$\left[gw_{T_R}\right.$/

and

$$\left[gw_{T_R}(q,\bar{x}_1,\bar{y}_1) + gw_{\Gamma_{T_R}}(q,\bar{x}_1,\bar{y}_1)\right.$$

$$= \left[\int_0^k \left\{\frac{1}{4\pi} \cdot \frac{-\bar{y}}{(1+\bar{y}^2)^{1/2}} \cdot q \cdot \left(\frac{1+\bar{y}^2}{1+k^2}\right)^{\frac{q-1}{2}} \cdot \left[(1-\bar{x}_1)-(\bar{y}-\bar{y}_1)\cot\beta(\bar{y})\right]\right.\right.$$

$$\left[I(\bar{y})\right]$$

$$+ \left\{(1+k^2)^{1/2} - \frac{(1+\bar{y}^2)^{q/2}}{(1+k^2)^{\frac{q-1}{2}}}\right\}\left[f_W(\bar{x} = (k-\bar{y})\cot\beta(\bar{y}) + 1, \bar{x}_1, \bar{y}_1, o)\right]$$

$$\left.\left. \cdot \left[-\cot\beta(\bar{y}) - (k-\bar{y})\operatorname{cosec}^2\beta(\bar{y})\frac{\partial\beta(\bar{y})}{\partial y}\right]\right\} d\bar{y}\right] .$$

$$\cdots (79)$$

Thus combining all the upwash terms in equations (69), (73), (77), the boundary condition of tangency of flow on this wing, equation (36), becomes

$$\sum_{p=0}^{n}\sum_{q=0}^{m} a_{2p+1,q} \cdot \left[aw_W(2p+1,q,\bar{x}_1,\bar{y}_1) + \left[aw_T(2p+1,q,\bar{x}_1,\bar{y}_1)\right.\right.$$

$$\left. + aw_{\Gamma_T}(2p+1,q,\bar{x}_1,\bar{y}_1)\right]$$

$$+ \sum_{q=1}^{\ell} g_q \cdot \left[gw_W(q,\bar{x}_1,\bar{y}_1) + \left[gw_T(q,\bar{x}_1,\bar{y}_1) + gw_{\Gamma_T}(q,\bar{x}_1,\bar{y}_1)\right]\right.$$

$$+ gw_{\Gamma_W}(q,\bar{x}_1,\bar{y}_1) \qquad = -\sin\alpha .$$

$$\cdots (80)$$

Next, the equations for satisfying the zero loading condition on the trailing edge are developed. In non-dimensional form, equation (8) becomes

$$\bar{\gamma}(1,\bar{y}) - \tan\beta(\bar{y}) . \bar{\delta}(1,\bar{y}) = 0 \qquad \cdots (81)$$

After substitution of the series for $\bar{\gamma}(x,\bar{y})$ and $\bar{\delta}(\bar{x},\bar{y})$ from equations (61) and (62), equation (81) becomes

$$\sum_{p=0}^{n} /$$

$$\sum_{p=0}^{n} \sum_{q=0}^{m} a_{2p+1,q} \cdot \left[a_y(2p+1,q,1,\bar{y}) - \tan\beta(\bar{y})\, a_\delta(2p+1,q,1,\bar{y}) \right]$$

$$- \sum_{q=1}^{\ell} g_q \left[g_y(q,1,\bar{y}) - \tan\beta(\bar{y}).\ g_\delta(q,1,\bar{y}) \right] = 0 \qquad \ldots (82)$$

The angle $\beta(\bar{y})$ in equation (82) is given by equation (6) which in non-dimensional form is

$$\tan\beta(\bar{y}) = \frac{v_T(1,\bar{y},o)}{V\cos\alpha + \bar{u}_T(1,\bar{y},o)} \qquad \ldots (83)$$

this involves the spanwise and streamwise velocities induced due to the two separated vortices.

For a specified leading edge vortex position over both S_W and S_T equations (80) and (82) can be set up. If $\beta(\bar{y})$ is assumed then equations (80) and (82) are linear in $a_{2p+1,q}$ and g_q ; so for a given number of coefficients the resulting simultaneous equations have to be satisfied at the same number of collocation points. In the present solution the number of collocation points over the wing is deliberately restricted, because the present intent is to investigate whether the approach leads to a sensible solution and also to find out the extent of the computational task relative to a limited number of collocation points. So in this study the upwash conditions are satisfied at 20 collocation points over half a wing (5 semi-spanwise points at 4 chordwise stations) while the condition of zero load on the trailing edge is satisfied at 5 trailing edge points along the semi-span, thus there are 20 coefficients $a_{2p+1,q}$ and 5 coefficients g_q to be found.

The distribution of the collocation points in spanwise direction is based on Multhopp's rule for odd number of points over a span. The chordwise distribution of these collocation stations is based on the intuitive feeling that as the effect of the wakes becomes more important towards the trailing edge region, the collocation points should be weighted towards the trailing edge. So somewhat arbitrarily the chordwise stations were distributed according to Multhopp's rule over a diameter of 2c for an even number of points. The full 20 collocation points thus chosen are shown in Fig. 4.

The positioning of 5 trailing edge points for the application of the boundary condition of zero load follows the same principle as the spanwise distribution of collocation points.

An iterative procedure suggests itself for solving the complete non-linear equations starting with an initially assumed value of $\beta(\bar{y})$. Equations (80) and (82) can then be solved and the resulting coefficients $a_{2p+1,q}$ and g_q can be substituted into equations (83) to give a new distribution of $\beta(\bar{y})$, so the process can be repeated. It was initially anticipated that once $\beta(\bar{y})$ had been iterated out the induced velocities at the assumed vortex position could be calculated and a new vortex position found from the equations (44) and (45), representing zero force on the vortex-cut arrangement.

As will be discussed later, this iteration cannot be used in such a simple fashion.

II.4.3 Evaluation of upwash integrals

Once the collocation points are decided upon it is necessary to evaluate the upwash integrals $aw_W(2p + 1,q,\bar{x}_1,\bar{y}_1)$, $\left[aw_T(2p + 1,q,\bar{x}_1,\bar{y}_1) + aw_{\Gamma_T}(2p + 1,q,\bar{x}_1,\bar{y}_1)\right]$, $gw_{\Gamma_W}(q,\bar{x}_1,\bar{y}_1)$, $\left[gw_T(q,\bar{x}_1,\bar{y}_1) + gw_{\Gamma_T}(q,\bar{x}_1,\bar{y}_1)\right]$ and $gw_W(q,x_1,y_1)$ in equation (80). Of these $aw_W(2p +1,q,\bar{x}_1,\bar{y}_1)$ and $gw_W(q,\bar{x}_1,\bar{y}_1)$ are functions involving double integration over the wing planform and need only be evaluated once, these are singular when $\bar{z}_1 = 0$ and require special care. The technique employed to deal with this type of integral is described in Appendix I. Of the remaining integrals, the integrals $gw_{\Gamma_W}(q,\bar{x}_1,\bar{y}_1)$ are functions of vortex position, the 'combined' integrals $\left[aw_T(2p + 1,q,\bar{x}_1,\bar{y}_1) + aw_{\Gamma_T}(2p + 1,q,\bar{x}_1,\bar{y}_1)\right]$ and $\left[gw_T(q,\bar{x}_1,\bar{y}_1) + gw_{\Gamma_T}(q,\bar{x}_1,\bar{y}_1)\right]$ depend on the deflection $\beta(\bar{y})$ of the vortex lines at the trailing edge as well as on the downstream vortex position. Since both the vortex position and the angle $\beta(\bar{y})$ vary during the iterative loops in the calculation, these last series of 'combined' integrals have to be re-evaluated several times. Fortunately these integrals are not singular.

Expressions for $\left[aw_T(2p + 1,q,\bar{x}_1,\bar{y}_1) + aw_{\Gamma_T}(2p + 1,q,\bar{x}_1,\bar{y}_1)\right]$ and $\left[gw_T(q,\bar{x}_1,\bar{y}_1) + gw_{\Gamma_T}(q,\bar{x}_1,\bar{y}_1)\right]$ given by reference to equations (78) and (79) are line integrals in terms of $\bar{y}$. After trying the 12-point, 24-point and 48-point Gaussian integration rules to a typical case it was decided that the 24-point rule was sufficient for the more general cases.

The expression for $gw_{\Gamma_W}(q,\bar{x}_1,\bar{y}_1)$ given by equation (73) involves some difficulty in accurate calculations using Gaussian quadrature methods especially in the region of the wing apex when $\bar{x}$ and $\bar{y}$ are both small. As a prelude, a test was made to evaluate numerically the upwash expression for a particular case of a pair of straight line vortices using Gaussian quadrature and to compare it with the exact analytical result. It was shown that splitting the integration ranges of 0 to 1 and 1 to infinity in equation (73) with small intervals was necessary. The $\bar{x}$ integration from 0 to 1 was split into a further 4 intervals, viz., 0 to 0·13, 0·13 to 0·25, 0·25 to 0·57, 0·57 to 1·0 , and four figure accuracy was obtainable using a 48-point Gaussian quadrature method for these four intervals. For the second range of $\bar{x}$ of 1 to infinity a 24-point modified Gauss-Laguerre[9] rule was found sufficient.

The induced velocities at the right-hand vortex $\bar{v}_1(\bar{x},\bar{y}_v(\bar{x}),\bar{z}_v(\bar{x}))$, $\bar{w}_1(\bar{x},\bar{y}_v(\bar{x}),\bar{z}_v(\bar{x}))$ depend on the wing vorticity, the trailing sheet vorticity and the left-hand vortex. As discussed in Section II.3 the effect of the right-hand vortex on itself has been neglected. The contribution due to the wing vorticity was evaluated by a 24 by 24-point double integration Gaussian method. The contribution due to the trailing sheet vorticity was evaluated using the same 24-point Gaussian quadrature technique as used in the calculations of the upwash due to the trailing sheet at the wing collocation points. For the effect of the left-hand vortex on the right-hand vortex, the range of integration was split up in the same manner as for upwash estimates.

II.5 Application of the theory

Initially it was anticipated that once the number and positioning of the collocation points had been decided that the numerical procedure would be as follows:

(1) The upwash integrals $aw_W(2p+1,q,\bar{x}_1,\bar{y}_1)$ and $gw_W(q,\bar{x}_1,\bar{y}_1)$ are evaluated.

(2) An initial position of the vortex is specified. A convenient starting point is the Brown and Michael value of the spanwise position $\bar{y}_v(\bar{x})$ and the height of the vortex $\bar{z}_v(\bar{x})$ together with their respective slopes $\frac{d\bar{y}_v(\bar{x})}{d\bar{x}}$ and $\frac{d\bar{z}_v(\bar{x})}{d\bar{x}}$, given in a tabular form. Over the wake aft of the trailing edge initially the vortices are taken to be straight and parallel to the free stream direction.

(3) A distribution of $\beta(\bar{y})$ is specified.

(4) The upwash integrals due to the vortices and the wake are evaluated.

(5) The coefficients of equation (82) expressing the zero load condition at a discrete number of points at the trailing edge are estimated.

(6) The solution of the 25 linear simultaneous equations (80) and (82) yield the values of unknowns $a_{2p+1,q}$ and g_q .

(7) $\beta(\bar{y})$ can be reassessed from the same position of the vortex specified in step (2) using the vortex strength calculated in step (6).

(8) Steps (4) to (7) are repeated to iterate out $\beta(\bar{y})$.

(9) The force on the main vortex is calculated using equations (44) and (45). If the force exceeds a prespecified 'tolerance' (factor F_{tol}) then the slopes of vortex geometry (equations (48) and (49)) are calculated within a prespecified tolerance (factor d_{tol}) . The 'corrections' to the slopes are then integrated to yield a new vortex position.

(10)/

(10) Steps (3) to (9) are repeated until the forces on the main vortex (step (9)) are below the prespecified 'tolerance' (factor F_{tol}).

Thus this method envisaged a significant iteration of $\beta(\bar{y})$ for each vortex position, but preliminary experience showed that iteration of $\beta(\bar{y})$ could not be divorced from the iteration of the vortex position. It is necessary for both iterations to progress side by side, and the following modifications have been developed:

Step (3) The distribution of $\beta(\bar{y})$ is so chosen that it never exceeds $\tan^{-1}(\bar{y})$. The reason for this empirical step is not evident but the calculations have shown that if $\beta(\bar{y})$ exceeds $\tan^{-1}(\bar{y})$ then the subsequent steps in calculations yield unrealistic negative values of vortex strength $\bar{\Gamma}_W(\bar{x})$ in the apex region of the wing.

Step (8) In step (7) a new distribution of $\beta(\bar{y})$ is calculated and compared with the initial value in step (3). If the new value is higher or equal to the initial value in step (2), then the calculation is taken directly forward to the stage of obtaining an estimate of the new vortex position (Steps (9) and (10)). If the new distribution of $\beta(\bar{y})$ is lower than the initial value in step (3), then the calculation is taken back to step (4) with an intermediate value of $\beta(\bar{y})$ as a part of an iterative procedure to iterate out $\beta(\bar{y})$ the empirical condition of ensuring $\beta(\bar{y})$ to be below the 'critical' $\tan^{-1}(\bar{y})$ curve need no longer be conformed to.

It is of interest to note the effect of $\beta(\bar{y})$ on the coefficients $a_{2p+1,q}$, g_q in equation (82) which expresses the zero load condition at a discrete number of points on the trailing edge including the centre and tip. It has been observed that if $\beta(\bar{y})$ never exceeds $\tan^{-1}(\bar{y})$ in step (2), then all the coefficients of equation (82) are positive. If $\beta(\bar{y})$ exceeds the 'critical' value of $\tan^{-1}(\bar{y})$, the coefficients are negative for collocation points at the trailing edge near the tip which leads to negative values for the vortex strength in the apex region.

This modified procedure is shown in a block diagram in Fig. 5.

II.5.1 Computer programmes

The application of the numerical procedure is by means of four general digital computer programmes written in Algol 60 language. During the development period the input was in form of punched 7-hole paper tape, but after development and during the 'production' period the programmes were loaded in the compiled form onto magnetic tape. The function of the programmes, which are tabulated in Table I, are:-

(1) Programme I evaluates the upwash coefficients $aw_W(2p+1, q, \bar{x}_1, \bar{y}_1)$ from a knowledge of the equations of the leading edges of the delta wing and the positions of the collocation 'mesh'. The upwash coefficients

need/

need only be calculated once and for all for a particular planform and a collocation 'mesh'.

(2) Programme II, similar in structure to Programme I, evaluates the upwash coefficients $gw_W(q,\bar{x}_1,\bar{y}_1)$ which again need to be calculated once and for all for a particular planform and a collocation 'mesh'.

(3) Programme III uses the upwash coefficients $aw_W(2p + 1,q,\bar{x}_1,\bar{y}_1)$ and $gw_W(q,\bar{x}_1,\bar{y}_1)$ calculated from Programmes I and II, the specified position of vortices, and the 'initial' value for the function $\beta(\bar{y})$ to calculate first the upwash coefficients due to the wake and then solves equations (80) and (82) for the values of unknown $a_{2p+1,q}$ and g_q. A 'new' value for the function $\beta(\bar{y})$ is estimated. The programme can be made to compare the two values 'initial' and 'new', of the function $\beta(\bar{y})$ and if required, it can iterate on $\beta(\bar{y})$, producing thus 'newer' sets for the values of unknowns $a_{2p+1,q}$ and g_q. This programme also includes the estimated lift distribution on the wing.

(4) Programme IV uses the calculated values of unknowns $a_{2p+1,q}$ and g_q from the Programme III and produces a 'new' vortex geometry within a specified small tolerance on the 'initial' geometry.

The details of the store and computation time requirements of the four computer programmes on the Atlas computer are shown in Table I. It may be observed that the compiling store and computing times are both reduced for the programmes loaded on magnetic tape. The reductions are very significant for running of Programme III, which with paper tape input would need almost the whole of the Atlas core store.

With the present collocation mesh (Fig. 4) Programme I and II take a total of about $2\frac{1}{2}$ hours to compute 400 $aw_W(2p + 1,q,\bar{x}_1,\bar{y}_1)$ and 100 $gw_W(q,x_1,\bar{y}_1)$ upwash coefficients. This represents the largest proportion of computer time for the overall development programme of the theory. During the initial phase of numerical work it was necessary to test various integration procedures in the calculation of upwash coefficients and therefore these two programmes were written to feature a certain amount of generality and adaptibility. This in turn has required large execution time on the computer. It is believed that starting afresh on another wing with the experience gained so far, it is possible to reprogram the inner and more repetitive calculation loops more efficiently and therefore reduce the computation times of Programmes I and II by a factor of 5.

The number of times the Programmes III and IV are required to be run performing the necessary iterations on $\beta(\bar{y})$ and the position of the vortices is dependent on 'initial' estimates and various 'tolerances'. Experience of the worked example (Section III) suggests something of the order of one $\beta(\bar{y})$ calculation (1 minute, execution time) for each of the 7 iterations in vortex position (2 minutes execution time for each iteration) starting with Brown and Michael values. It is anticipated that as the experience with the programme grows, improved initial estimates with 'proper' tolerances would reduce the computation time requirements.

III. A Worked Example

The theory has been applied to the case of a delta wing of aspect ratio 1 at incidence 0·25 radian. The initial vortex position was based on that calculated by Randall[10] using Brown and Michael theory; this position is shown as 0 in Fig. 6. The assumed distribution of $\beta(\bar{y})$ chosen such that it did not exceed 'critical' $\tan^{-1}(\bar{y})$ curve is shown in Fig. 7b. With this information the coefficients $a_{2p+1,q}$ and g_q were evaluated. At this stage the vortex strength $\bar{\Gamma}_W(\bar{x})$ which is easier to visualise, is shown; its first value denoted as 0 is indicated in Fig. 7a. It shows a peak in the region near the apex, hence the feeding vorticity $d\bar{\Gamma}_W(\bar{x})/d\bar{x}$ is positive in the region near the apex but mostly negative over the rest of the wing. The 'calculated' $\beta(\bar{y})$ curve was found to be higher than the initial guessed $\beta(\bar{y})$ curve (Fig. 7b) so the calculation was taken to the next stage of obtaining a 'new' vortex position.

The force on the vortex was calculated as discussed in Section II.3 and two new positions 1 and 1' (shown in Fig. 6) based on tolerances $d_{tol} = 0{\cdot}005$ and $0{\cdot}01$ respectively on the slopes of the initial position 0 were determined. Two different 'tolerance' were introduced mainly to obtain some idea of their influence on the vortex movements. The general trends in the vortex movement, shown by positions 1 and 1', relative to position 0, are outwards and downwards in the forward part of the wing and inwards and upwards over the rear part of the wing. Aft of the wing the tendency for the vortices is to become parallel to each other. These positions 1 and 1' with a suitable $\beta(\bar{y})$ distribution (bounded by the critical $\tan^{-1}(\bar{y})$ curve) were then used to solve for the unknowns $a_{2p+1,q}$ and g_q. The vortex strength based on position 1 is shown in Fig. 7a (the curve for 1' is similar); it shows less peaks in the apex region than the previous estimate based on the position 0 thus increasing the feeding vorticity in the rear positions of the wing. Also the difference between the two $\beta(\bar{y})$ curves, 'initial' and 'calculated', decreased slightly for the vortex position 1 (Fig. 7c) when compared with those for vortex position 0 (Fig. 7b).

The calculation was continued by deriving a new vortex position 2 from vortex position 1' within a tolerance of 0·01. Using vortex position 2, and a guessed distribution $\beta(\bar{y})$ the vortex strength $\bar{\Gamma}_W(\bar{x})$ (Fig. 7a) the wing vorticity distribution and a new $\beta(\bar{y})$ distribution were calculated (Fig. 7d). All of these quantities showed a much improved character and the feeding vorticity was for the first time positive over the whole of the wing.

It seems reasonable to stipulate that tolerance d_{tol} should be reduced as the iterations progress and consequently the next vortex position 3 (Fig. 6) was developed by a further iteration on the vortex position 2 with tolerance $d_{tol} = 0{\cdot}005$, and the results of vortex strength and $\beta(\bar{y})$ were observed to maintain the established trends.

Further/

Further iterations of this example were not completed because the time allotted to the project ran out.

However, there appears to be convergence of the vortex strength $\bar{\Gamma}_W(\bar{x})$ and of the vortex positions but the convergence of the zero load condition on the trailing edge indicated by the $\beta(\bar{y})$ curves, is not too successful. The vortex positions in Fig. 6 are more 'kinky' than might be intuitively expected to occur in practice but it is probable that this aspect is a reflection of the small number of chordwise collocation points used here. Also it is known from experience with the slender wing Brown and Michael model that at least seven spanwise collocation points are needed to give a numerical solution close to the analytical solution, in the present three-dimensional problem only 5 spanwise points have been taken.

It has already been noted that with the original vortex position over the wing assumed on the basis of the "two-dimensional" theory of Brown and Michael, the vortex strength $\bar{\Gamma}_W(\bar{x})$ over the front part of the wing showed a peak, and the corresponding strength of the cut $d\bar{\Gamma}_W(\bar{x})/d\bar{x}$ was found to be positive only in the forward part of the wing, and negative over most of the rear part. The peaks in the vortex strength over the front of the wing reduced as the vortex position was successively moved outboard and downwards over the forward half of the wing and inboard and upwards over the rear part of the wing.

Mathematically the effect of $\bar{y}_g$, which is much more dominant than $\bar{\delta}_g$, is to induce upward velocity over the forward part of the wing and downward velocity towards the rear part of the wing. To balance this effect, the main vortex has to be aligned closer to the wing surface over the forward part of the wing, and further away from the surface over the rear part of the wing. The movement of the vortex over the front part of the wing is downward, and in accordance with the usual Brown and Michael trends, there is an outward movement of the vortex.

IV. Comparison of the Method with Experimental Results

The calculated lift distribution for the flat delta wing at incidence of 0·25 radian has been compared in Fig. 8 with experimental results obtained at Queen Mary College (so far unpublished).

First the overall force coefficients are

$$C_{L_{\text{Experiment}}} = 0{\cdot}495$$

$$C_{L_{\text{Theory}}} = 0{\cdot}45$$

while the centres of pressure are

$$\bar{x}_{c_{p_{\text{Experiment}}}} = 0{\cdot}61$$

$$\bar{x}_{c_{p_{\text{Theory}}}} = 0{\cdot}60$$

The agreement of these overall features is encouraging.

For/

For the load distributions, in Fig. 8, it should be noted that the theoretical curves are not at the same chordwise station as the experimental ones. The general trends seem to be predicted. The fall off of lift towards the trailing edge is reasonable. Along the centreline the theoretical lift distribution is in remarkable agreement with experiment. The characteristic features of the basic Brown and Michael model where the suction peaks are outboard of the experimental peaks is still present as might be expected.

The theoretical distribution at the leading edge shows a finite load which is proportional to the feeding vorticity $d\bar{\Gamma}_W(\bar{x})/d\bar{x}$; this is seen to tend to zero at the tip of the wing in accordance with the boundary conditions.

Slight 'up-kinks' appear near the leading edge on the last two chordwise stations. These are not reasonable but they are probably due to the restriction of the number of terms in the series expansions.

V. Concluding Remarks

The theoretical approach outlined in this paper is an attempt to satisfy the zero load trailing edge condition on a delta wing in the presence of a separated vortex sheet from the leading edge of slender wings.

The approach has been restricted to a simple model employing a smallish number of collocation points over the wing. Even though a complete iteration has not been achieved the main features of the loading predicted by the theory tie in encouragingly with the experimental trends.

The application of the mathematical technique, apart from the numerical aspect, in solving this particular non-linear problem by iteration has shown up some interesting aspects, in particular the interaction of the two iterative procedures relating $\beta(\bar{y})$ and the vortex position.

The numerical aspect has involved complicated programming to enable the computation time to be kept to a minimum at every stage, especially where the integration has occurred of a function which includes a variable index but constant limits of integration.

The estimated computation time for the present application is of the order of half an hour on 'Atlas' for each incidence with a reasonable initial assumption of the position of main vortices. It is estimated that the use of more collocation points would not greatly increase the computation per incidence time provided some of the numerical techniques could be further refined and if possible, use is made of machine code procedures for the 'inner' or more repetitive operations.

To proceed further in the development of the present method, improving the efficiency of the integration procedure, searching for faster iterative dodges, coping with more and more collocation points, the final result will only marginally be a better representation of the physical flow. By incorporating the Brown and Michael model into the lifting surface theory framework all the inherent faults of the model will still remain; the leading edge vortices will be too far outboard, finite loads at the wing leading edge will remain, and the suction peaks on the wing upper surface will be too high. Admittedly it is possible to superimpose on the theoretical results empirical factors based on the large fund of experience now available on the loadings of these types of wings. But the question which needs at least recognising before proceeding further is whether it is worthwhile to incur large expenses utilising the resources of a large computer for long periods when for the practical application empirical factors might have to be thrown in at the end somewhat arbitrarily. It is the hope of the authors that the present paper throws some light on this particular wing problem, and that some of the implications and trends have been established; what happens next depends largely on the reaction which this paper arouses.

References/

References

No.	Author(s)	Title, etc.
1	R. Legendre	Flow in the Neighbourhood of the Apex of a Highly Swept Wing at Moderate Incidences. La Recherche Aeronautique 30, 1951, 31 and 35, 1953. Translation A.R.C.16 796, 1954.
2	C. F. Brown and W. H. Michael	On Slender Wings with Leading Edge Separation. NACA TN 3430, 1955.
3	K. W. Mangler and J. H. B. Smith	A Theory pf Slender Delta Wings with Leading Edge Separation. RAE Tech. Note Aero.2442, 1956. A.R.C.18 757.
	and	Calculation of the Flow Past Slender Delta Wings with Leading Edge Separation. RAE Report Aero. 2593, 1957. A.R.C.19 634.
	also	Proc. Roy. Soc. A. Vol. 251 (pp.200-217), 1959.
4	E. C. Maskell	Some Recent Developments in the Study of Leading Edge Vortices. Proceedings of International Council of Aeronautical Sciences, Stockholm, 1962.
5	J. H. B. Smith	Improved Calculation of Leading Edge Separation from Slender Wings. RAE Tech. Report 66070, 1966.
6	K. Gersten	Calculation of Non-Linear Aerodynamic Derivatives of Aeroplanes. AGARD Report 342, 1961.
7	H. C. Garner and D. E. Lehrian	Non-Linear Theory of Steady Forces on Wings with Leading-Edge Flow Separation. A.R.C. R.& M. 3375, 1963.
8	A. H. Sacks. J. N. Nielson and F. K. Goodwin	A Theory for the Low Speed Aerodynamics of Straight and Swept Wings with Flow Separation. VIDYA Report 91, 1963.
9	V. I. Krylov	Approximate Calculation of Integrals. Macmillan, 1962.
10	D. G. Randall	Oscillating Slender Wings in the Presence of Leading-Edge Separation. RAE Report Structures 286, 1963. A.R.C.24 929.
11	G. E. Bartholomew	Numerical Integration over the Triangle. M.T.A.C. Vol.XIII (pp.295-298), 1959.
12	A. H. Stroud and D. Secrest	Gaussian Quadrature Formulae. Prentice Hall, 1966.

APPENDIX I

Calculation of Upwash Integrals

The upwash due to vorticity over the wing surface is given by equations (13) and (69) as

$$\bar{w}_W(\bar{x}_1,\bar{y}_1,o) = \frac{1}{4\pi} \iint\limits_{\substack{S_W \\ \bar{z}_1 \to 0}} \frac{(\bar{x}-\bar{x}_1)\,\bar{\gamma}(\bar{x},\bar{y}) - (\bar{y}-\bar{y}_1).\,\bar{\delta}(\bar{x},\bar{y})}{[(\bar{x}-\bar{x}_1)^2 + (\bar{y}-\bar{y}_1)^2 + \bar{z}_1^2]^{3/2}}\, d\bar{x}\, d\bar{y}$$

$$= \sum_{p=0}^{n} \sum_{q=0}^{m} a_{2p+1,q} \cdot aw_W(2p+1,q,\bar{x}_1,\bar{y}_1) + \sum_{q=1}^{\ell} g_q \cdot gw_W(q,\bar{x}_1,\bar{y}_1) \; .$$

when the series for $\bar{\gamma}$ and $\bar{\delta}$ are substituted.

The problem is to obtain the upwash coefficients $gw_W(q,\bar{x}_1,\bar{y}_1)$ and $aw_W(2p+1,q,\bar{x}_1,\bar{y}_1)$ for various values of the indices p,q $(o \leqslant p \leqslant n$, $o \leqslant q \leqslant m)$ and various values of the positions $\bar{x}_1,\bar{y}_1$, corresponding to each of the collocation points on the wing surface. Since the expressions for $\bar{\gamma}(\bar{x},\bar{y})$ and $\delta(\bar{x},\bar{y})$ contain powers of $\bar{x}$ and $\bar{y}$ it will be sufficient to discuss the procedure corresponding to just one term of the above two series.

Taking the case of $aw_W(2p+1,q,\bar{x}_1,\bar{y}_1)$ the expression is expanded to reduce the order of singularity. Thus

$$aw_W(2p+1,q,\bar{x}_1,\bar{y}_1) = \frac{1}{4\pi} \iint\limits_{\substack{S_W \\ \bar{z}_1 \to 0}} \Big\{ (\bar{x}-\bar{x}_1)\,[a_\gamma(2p+1,q,\bar{x},\bar{y}) - a_\gamma(2p+1,q,\bar{x}_1,\bar{y}_1)]$$

$$- (\bar{y}-\bar{y}_1)\,[a_\delta(2p+1,q,\bar{x},\bar{y}) - a_\delta(2p+1,q,\bar{x}_1,\bar{y}_1)] \Big\} .$$

$$\frac{1}{[(\bar{x}-\bar{x}_1)^2 + (\bar{y}-\bar{y}_1)^2 + \bar{z}_1^2]^{3/2}} \cdot d\bar{x}.d\bar{y} \; .$$

$$+ \frac{1}{4\pi} a_\gamma(2p+1,q,\bar{x}_1,\bar{y}_1) \iint\limits_{\substack{S_W \\ z_1 \to 0}} \frac{(\bar{x}-\bar{x}_1)}{[(\bar{x}-\bar{x}_1)^2 + (\bar{y}-\bar{y}_1)^2 + \bar{z}_1^2]^{3/2}}\, d\bar{x}\, d\bar{y}$$

$$+ \frac{1}{4\pi} a_\delta(2p+1,q,\bar{x}_1,\bar{y}_1) \iint\limits_{\substack{S_W \\ \bar{z}_1 \to 0}} \frac{-(\bar{y}-\bar{y}_1)}{[(\bar{x}-\bar{x}_1)^2 + (\bar{y}-\bar{y}_1)^2 + \bar{z}_1^2]^{3/2}}\, d\bar{x}\, d\bar{y}. \qquad \ldots \text{(A1)}$$

The/

The last two integrals in the above equation can be reduced analytically to yield the following results with $\bar{z}_1 = 0$

$$\int_{-k}^{+k}\int_{\left|\frac{\bar{y}}{k}\right|}^{1} \frac{\bar{x} - \bar{x}_1}{[(\bar{x} - \bar{x}_1)^2 + (\bar{y} - \bar{y}_1)^2]^{3/2}} \, d\bar{x} \, d\bar{y}$$

$$= \sin h^{-1} \frac{k - \bar{y}_1}{1 - \bar{x}_1} + \sin h^{-1} \frac{-k - \bar{y}_1}{1 - x_1}$$

$$+ \frac{k}{(1 + k^2)^{1/2}} \left[\sin h^{-1} \frac{(k^2 + 1) - (k\bar{y}_1 + x_1)}{[k^2 + 1)(\bar{x}_1^2 + \bar{y}_1^2) - (k\bar{y}_1 + \bar{x}_1)^2]^{1/2}} - \sin h^{-1} \frac{-(k\bar{y}_1 + \bar{x}_1)}{[(k^2 + 1)(\bar{x}_1^2 + \bar{y}_1^2) - (k\bar{y}_1 + \bar{x}_1)^2]^{1/2}} \right]$$

$$+ \frac{k}{(1 + k^2)^{1/2}} \left[\sin h^{-1} \frac{-(k\bar{y}_1 - \bar{x}_1)}{[(k^2 + 1)(\bar{x}_1^2 + \bar{y}_1^2) - (k\bar{y}_1 - \bar{x}_1)^2]^{1/2}} - \sin h^{-1} \frac{-(k^2 + 1) - (k\bar{y}_1 - \bar{x}_1)}{[(k^2 + 1)(\bar{x}_1^2 + \bar{y}_1^2) - (k\bar{y}_1 - \bar{x}_1)^2]^{1/2}} \right]$$

... (A2)

and/

and
$$\int_0^c \int_{-kx}^{+kx} \frac{-(\bar{y}-\bar{y}_1)}{[(\bar{x}-\bar{x}_1)^2+(\bar{y}-\bar{y}_1)^2]^{3/2}} \, d\bar{x}\, dy$$

$$= \frac{-1}{(k^2+1)^{1/2}} \left[\sin h^{-1} \frac{(k^2+1)-(\bar{x}_1+k\bar{y}_1)}{[(k^2+1)(\bar{x}_1^2+\bar{y}_1^2)-(\bar{x}_1+k\bar{y}_1)^2]^{1/2}} \right.$$

$$\left. - \sin h^{-1} \frac{-(\bar{x}_1+k\bar{y}_1)}{[(k^2+1)(\bar{x}_1^2+\bar{y}_1^2)-(\bar{x}_1+k\bar{y}_1)^2]^{1/2}} \right]$$

$$+ \frac{1}{(k^2+1)^{1/2}} \left[\sin h^{-1} \frac{(k^2+1)-(\bar{x}_1-k\bar{y}_1)}{[(k^2+1)(\bar{x}_1^2+\bar{y}_1^2)-(\bar{x}_1-k\bar{y}_1)^2]^{1/2}} \right.$$

$$\left. - \sin h^{-1} \frac{-(\bar{x}_1-k\bar{y}_1)}{[(k^2+1)(\bar{x}_1^2+\bar{y}_1^2)-(\bar{x}_1-k\bar{y}_1)^2]^{1/2}} \right] . \qquad \cdots \text{(A3)}$$

The first double integral in equation (A1) features an integrand which is zero at the point $\bar{x} = \bar{x}_1$ and $\bar{y} = \bar{y}_1$ for all values of $\bar{z}_1$. However, the behaviour of the integrand in the neighbourhood of this point is dependent on $\bar{z}_1$ and as $\bar{z}_1$ decreases, sharper variations of the integrand are shown across the point $(\bar{x}_1, \bar{y}_1)$. This double integral therefore necessitates an efficient computing technique with $\bar{z}_1$ chosen in such a way that it makes only a small difference in say the fifth or sixth figure of the overall value of the integral and thus a small value for $\bar{z}_1 (\simeq 1 \times 10^{-9})$ may be pre-specified.

In an effort to relate the efficiency of computation with accuracy obtainable for numerical integration of the double integral, a number of methods were investigated. One of the methods considered was that of double integration over a triangle developed by Bartholomew[11]. Briefly stated the integration of a function over a triangle can be calculated by summing the function evaluated at mid points of its sides with unity weighting. Thus the first approximation to the value of integral involves evaluation on the integrand at 3 points (Fig. 9) and second approximation involves 9 such points. These points for the second approximation, however, do not include the points of evaluation for the first approximation and the method therefore can not be set up efficiently to work successively to a desired accuracy. The 'order' of the approximation has therefore to be pre-specified. It was discovered that

the/

the seventh-order approximation which involves 6240 evaluations of the integrand was capable of producing results to about 5 figures accuracy for the upwashes near the centre line of the wing but this accuracy reduced somewhat if the upwash calculation were required near the leading edges.

The second method considered was of the application of Gaussian methods of quadrature[12] over the delta wing sub-divided as shown in Fig. 10 with a higher density of points for evaluation of the integrand in the neighbourhood of point $\bar{x} = \bar{x}_1$ and $\bar{y} = \bar{y}_1$. Three cases of Gaussian methods using 12, 24 and 48 points in each interval were further investigated and the last one, using 48 points over an interval, was eventually adopted for double integration over the delta wing.

APPENDIX II

Reduction of Integral $[I(\bar{y})]$ (Equation 18)

By definition

$$[I(\bar{y})] = \int_{\bar{y}}^{k} \frac{1}{[\{(\bar{y}_\ell - \bar{y})\cot\beta(\bar{y}) + (1-\bar{x}_1)\}^2 + (\bar{y}_\ell - \bar{y}_1)^2 + \bar{z}_1^2]^{3/2}}\, d\bar{y}_\ell$$

$$= \int_{\bar{y}}^{k} \frac{d\bar{y}_\ell}{\left[\begin{array}{l}\bar{y}_\ell^2\{1+\cot^2\beta(\bar{y})\} + \bar{y}_\ell\{-2\bar{y}\cot^2\beta(\bar{y}) + 2(1-\bar{x}_1)\cot\beta(\bar{y}) - 2\bar{y}_1\} \\ \quad + \{(1-\bar{x}_1^2) + \bar{y}^2\cot^2\beta(\bar{y}) - 2(1-\bar{x}_1)\cot\beta(\bar{y})\,\bar{y} + \bar{y}_1^2 + \bar{z}_1^2\}\end{array}\right]^{3/2}}$$

This is recognised as a standard form and on integration gives

$$[I(\bar{y})] = \left[\frac{\cot^2\beta(\bar{y})(\bar{y}_\ell - \bar{y}) + (\bar{y}_\ell - \bar{y}_1) + \cot\beta(\bar{y})(1-\bar{x}_1)}{\left\{\begin{array}{l}[\{(1-\bar{x}_1) + \cot\beta(\bar{y})(\bar{y}_1 - \bar{y})\}^2 + \{1+\cot^2\beta(\bar{y})\}\bar{z}_1^2] \\ \quad \times [\{(1-\bar{x}_1) + \cot\beta(\bar{y})(\bar{y}_\ell - \bar{y})\}^2 + (\bar{y}_\ell - \bar{y}_1)^2 + \bar{z}_1^2\}]^{1/2}\end{array}\right\}}\right]_{\bar{y}}^{k}$$

$$= \frac{1}{[\{(1-\bar{x}_1) + \cot\beta(\bar{y})(\bar{y}_1 - \bar{y})\}^2 + (1+\cot^2\beta(\bar{y}))\bar{z}_1^2]} \cdot$$

$$\left[-\frac{(\bar{y} - \bar{y}_1) + \cot\beta(\bar{y})(1-\bar{x}_1)}{[(1-\bar{x}_1)^2 + (\bar{y}-\bar{y}_1)^2 + \bar{z}_1^2]^{1/2}}\right.$$

$$\left. + \frac{(\cot^2\beta(\bar{y}) + 1)(k-\bar{y}) + \cot\beta(\bar{y})(1-\bar{x}_1)}{[\{(1-\bar{x}_1) + (k-\bar{y})\cot\beta(\bar{y})\}^2 + (k-\bar{y}_1)^2 + \bar{z}_1^2]^{1/2}}\right].$$

TABLE I/

BMG.

TABLE I

Details of Computation Store and Time Requirement of the Four Computer Programmes on Atlas

Programme	Computation Store		Time Sec.		Execution Time for
	Compiling	Execution	Compiling	Execution	
I	80 40*	40	12 1*	18	One $aw_W(2p + 1, q, \bar{x}_1, \bar{y}_1)$ (For present 'collocation mesh' : 400 required)
II	80 40*	40	12 1*	15	One $gw_W(q, \bar{x}_1, \bar{y}_1)$ (For present 'collocation mesh' : 100 required)
III	165 80*	80	40 1*	60	One value of $\beta(y)$ at a given vortex position
IV	120 70*	60	20 1*	140	Prediction of new vortex geometry specified at 15 points

*Programme loaded on magnetic tape for production runs

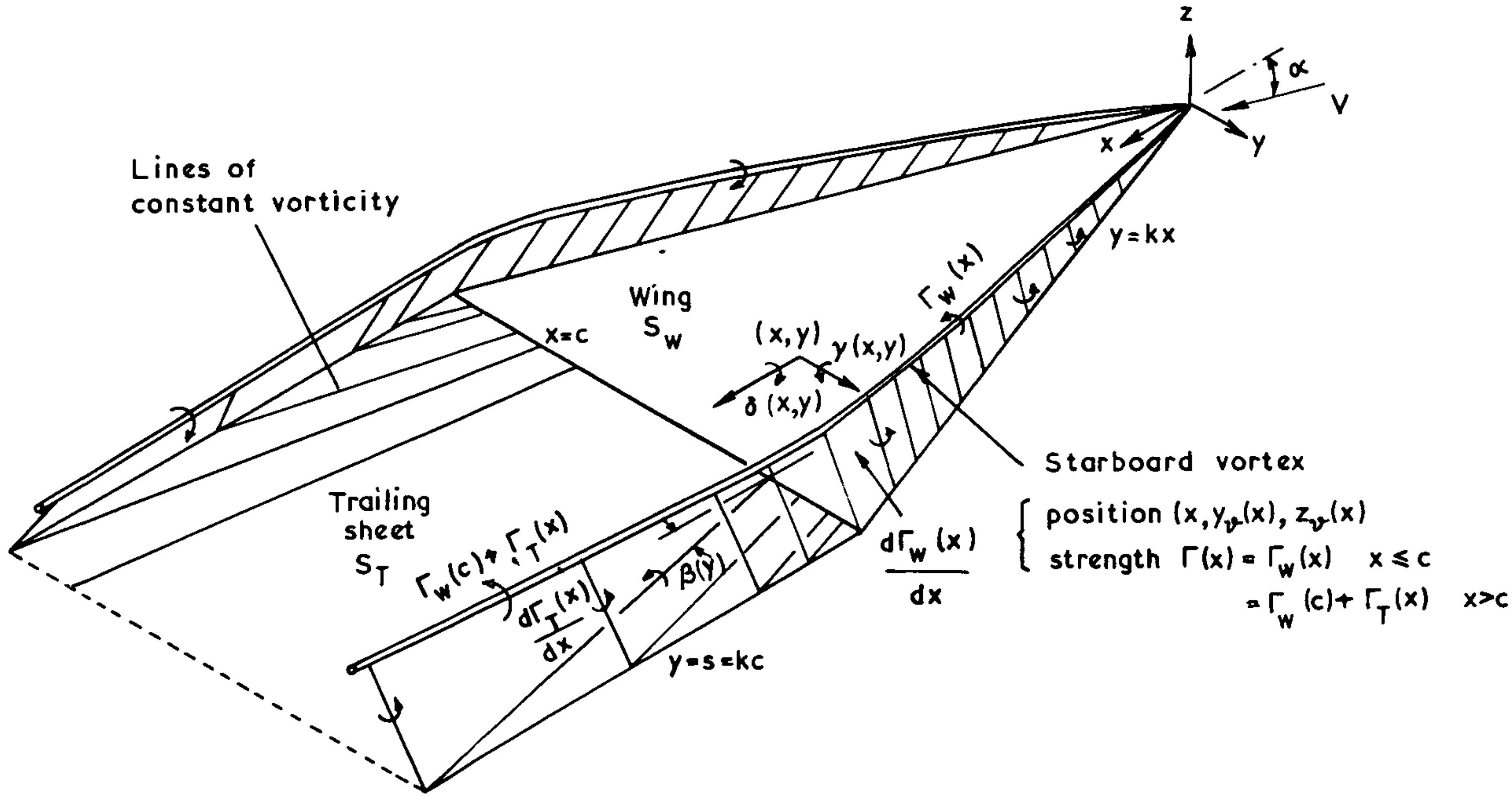

Theoretical model

FIG. 1

FIG. 2

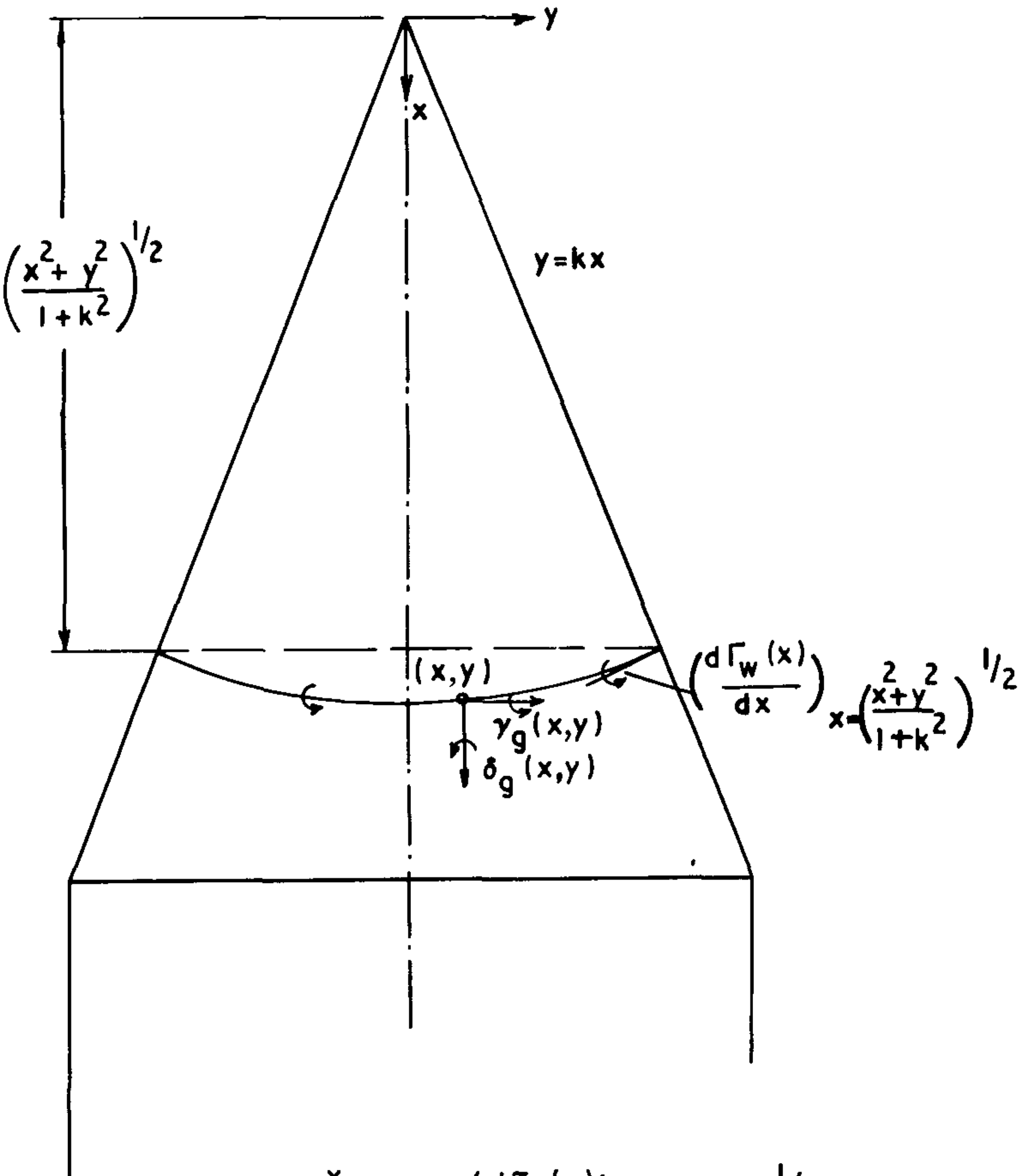

$$\gamma_g(x,y) = \frac{x}{(x^2+y^2)^{1/2}} \left(\frac{d\Gamma_w(x)}{dx}\right)_{x=\left(\frac{x^2+y^2}{1+k^2}\right)^{1/2}}$$

$$\delta_g(x,y) = \frac{y}{(x^2+y^2)^{1/2}} \left(\frac{d\Gamma_w(x)}{dx}\right)_{x=\left(\frac{x^2+y^2}{1+k^2}\right)^{1/2}}$$

Equilibrium of vorticity at the leading edge

FIG. 3

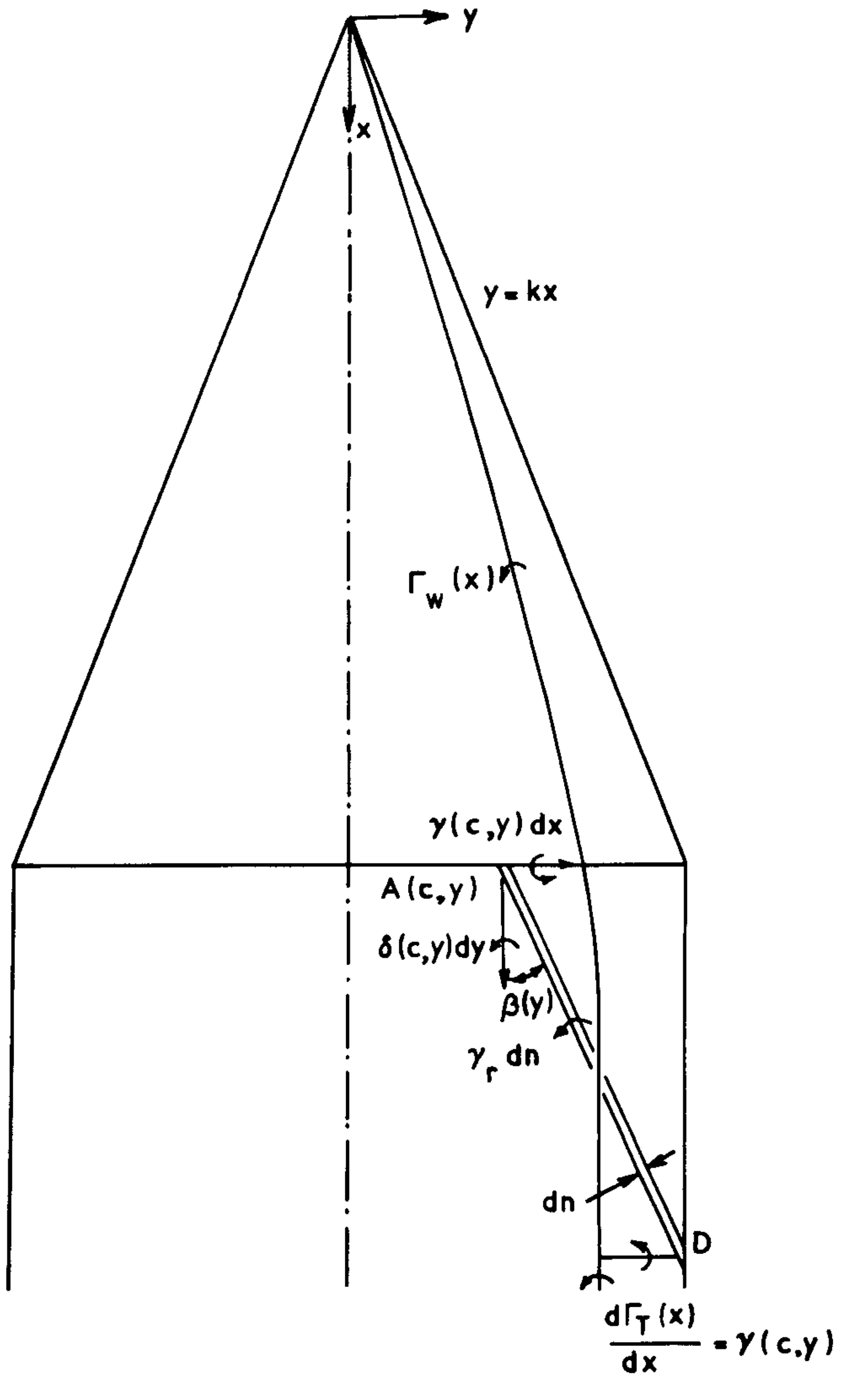

Simplified wake

FIG. 4

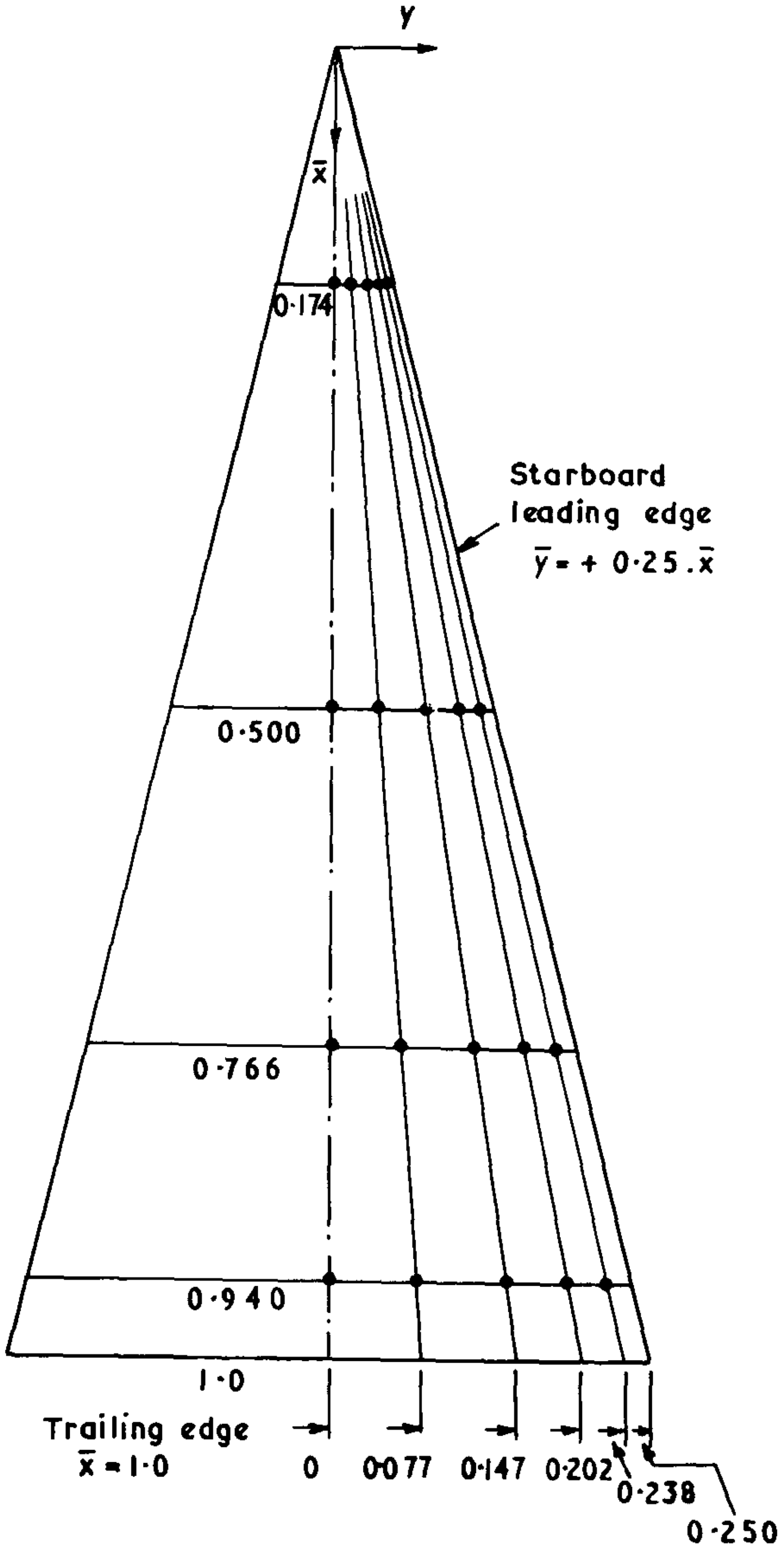

Wing collocation points

FIG. 5

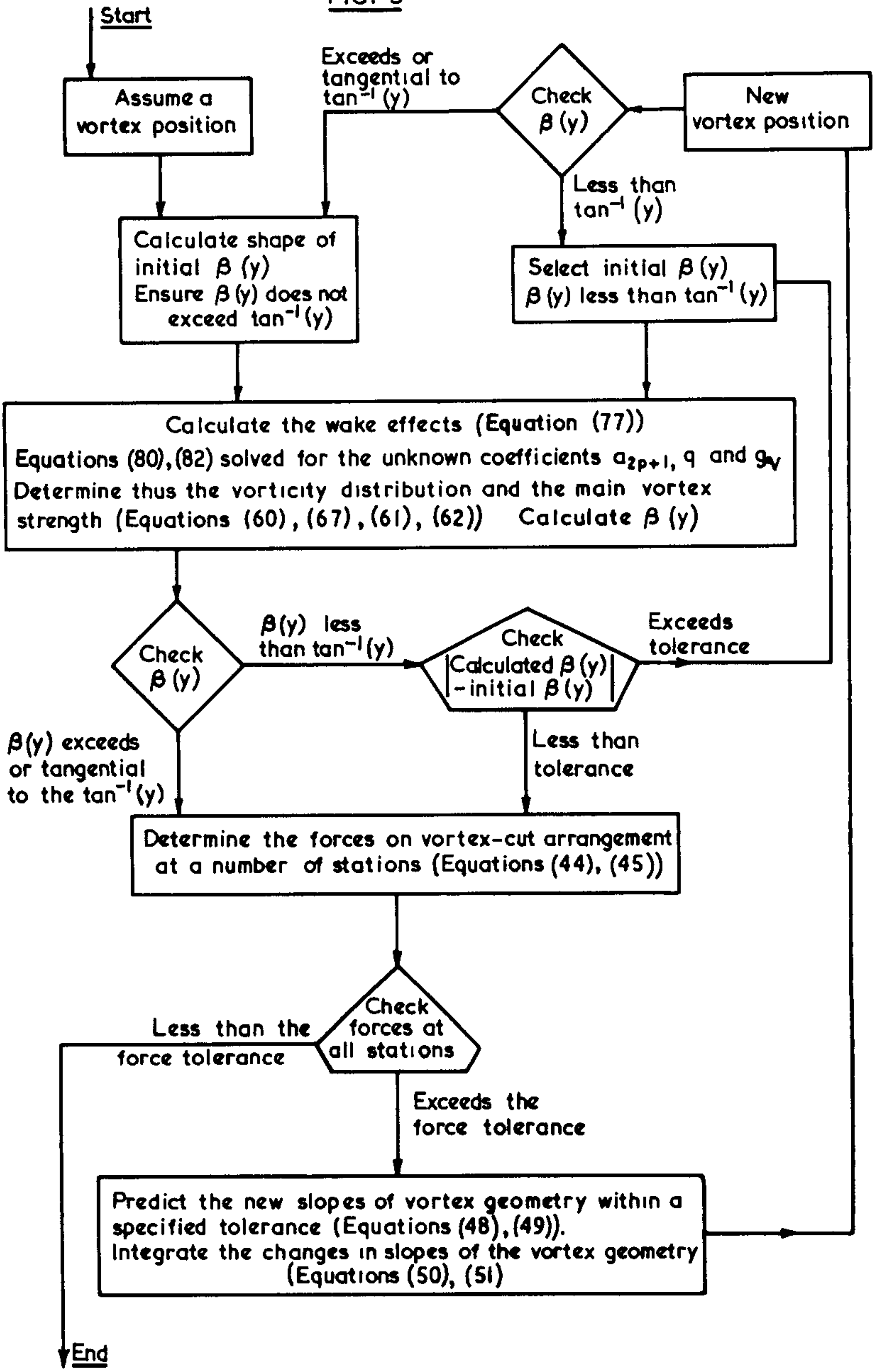

Proposed method for calculation of present theory

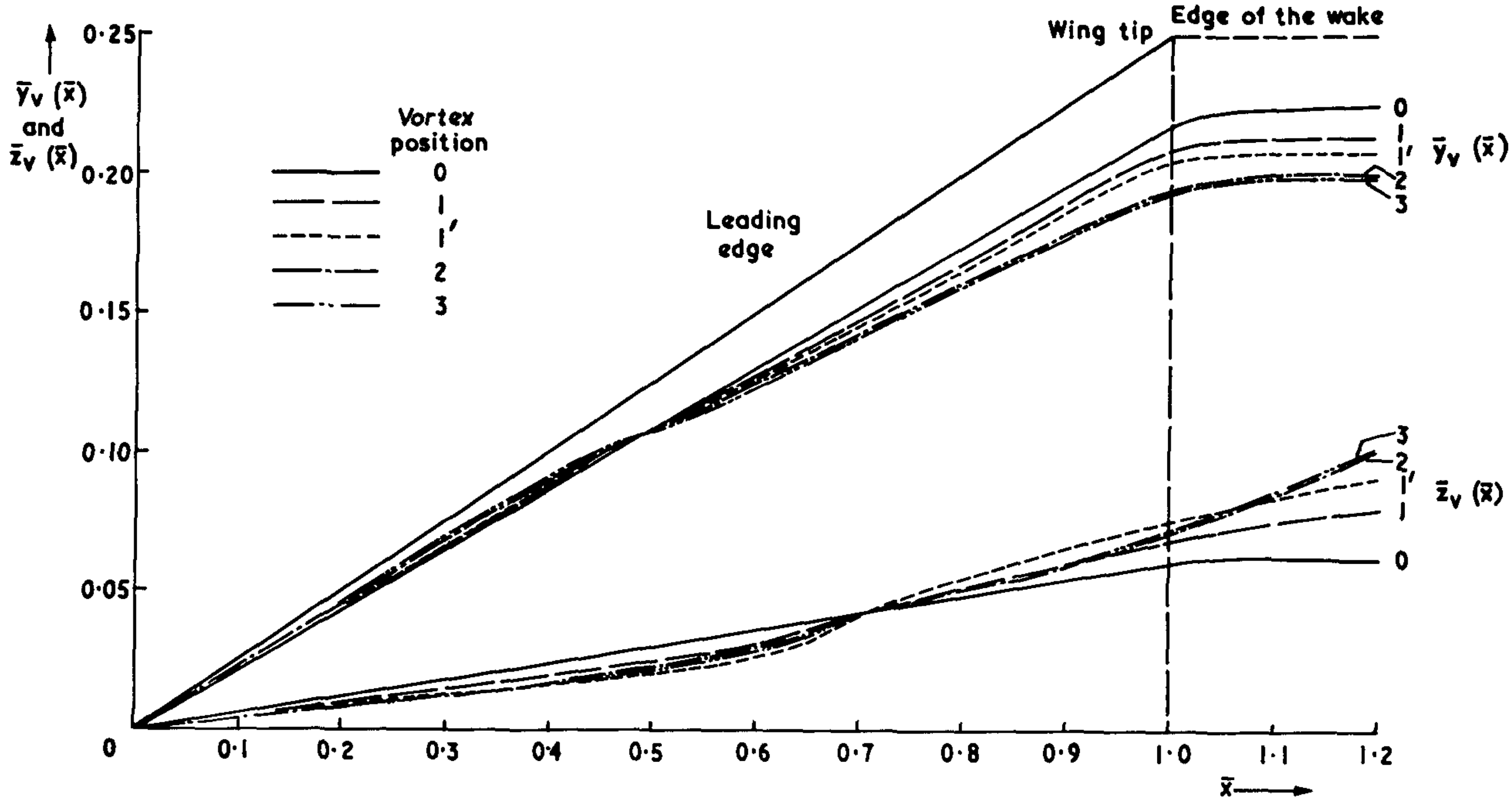

Vortex positions at various stages of solution

FIG. 6

FIG. 7

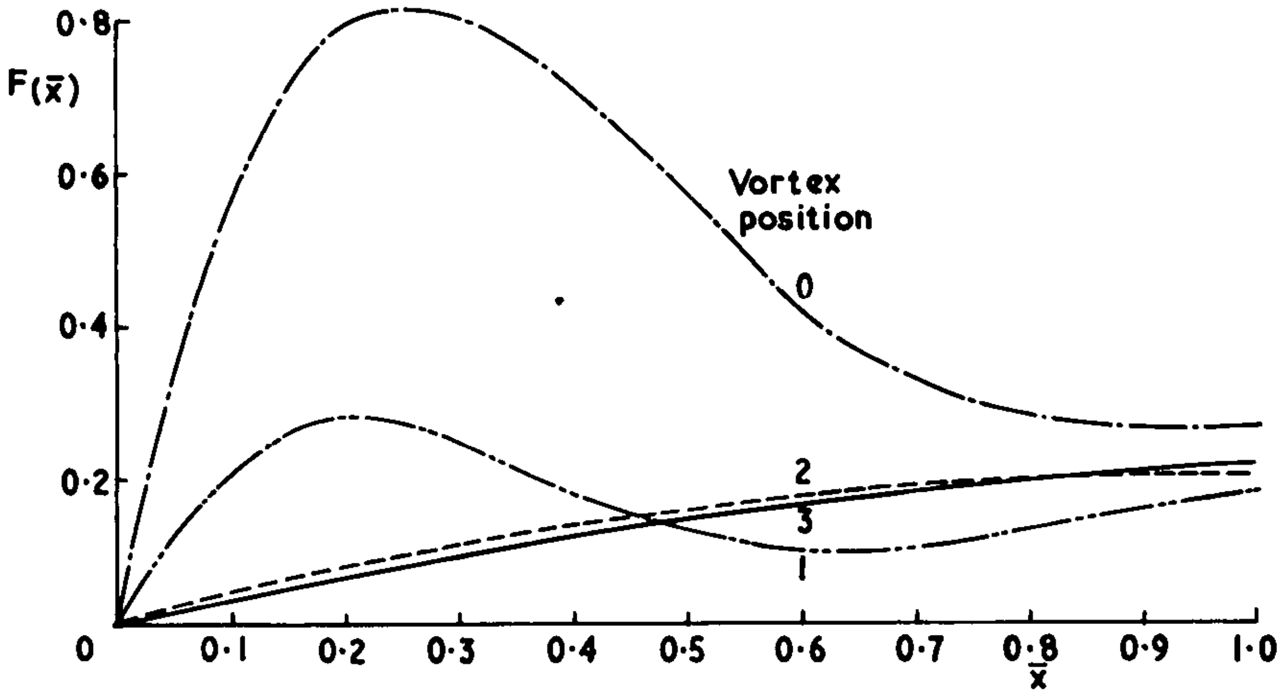

(a) Vortex strengths

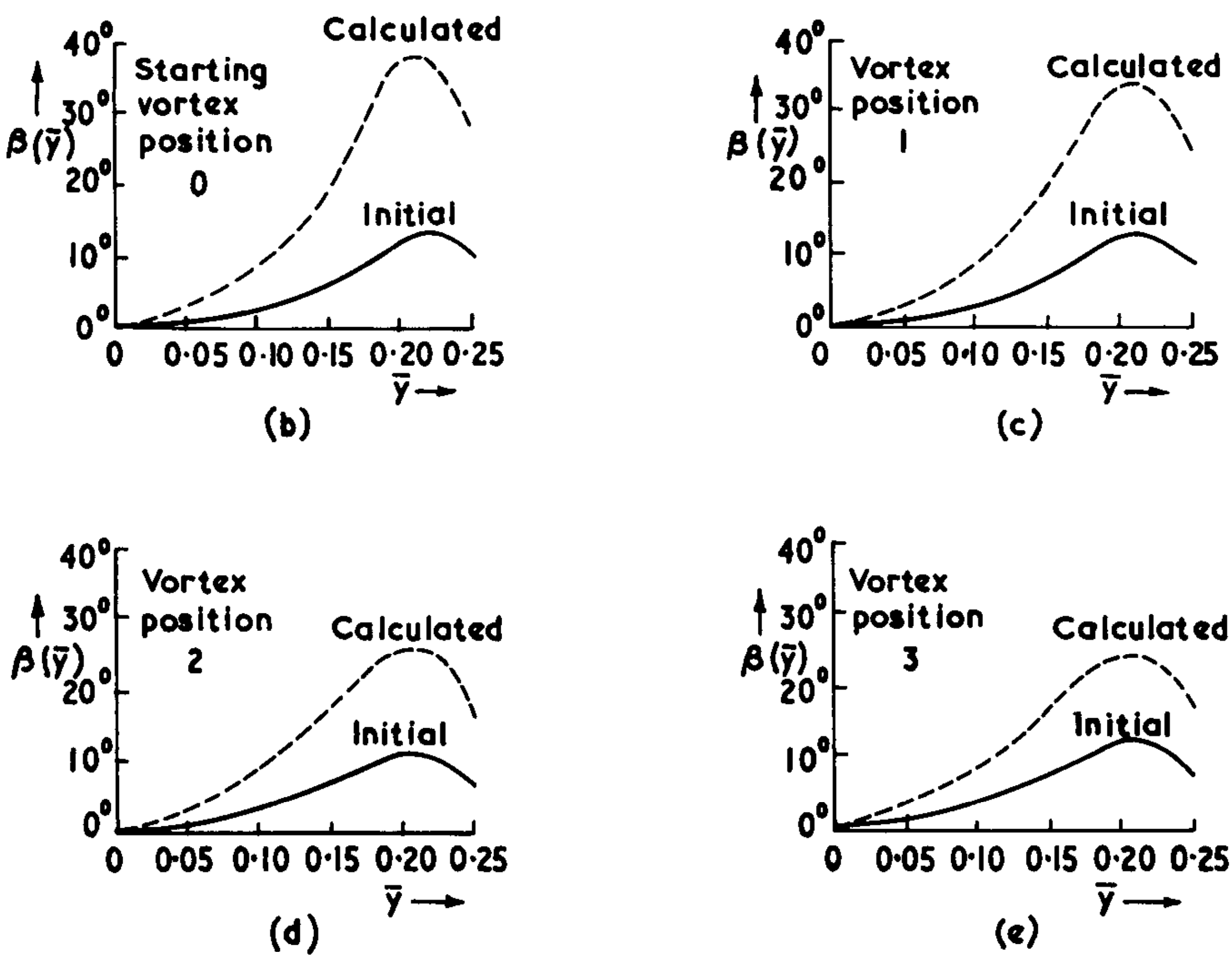

(b)-(e) Variation of β (y)

FIG. 8

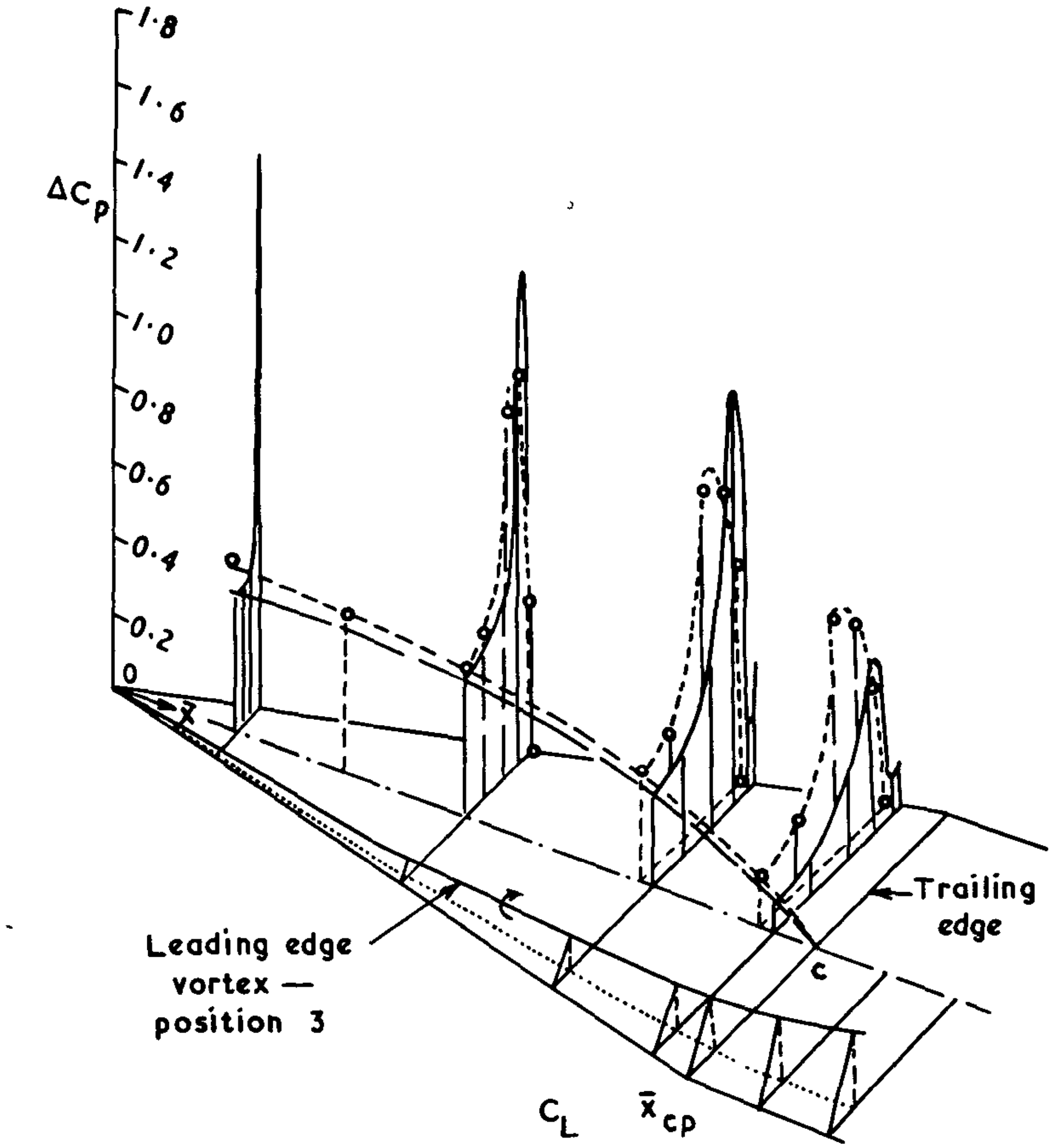

		C_L	$\bar{x}_{cp}$
- - -o- - -	Experiment	0·495	0·61
———	Present theory	0·46	0·60

Comparison of present theory and experiment for a flat delta wing of aspect ratio 1 at incidence of 0·25 rad.

FIG. 9

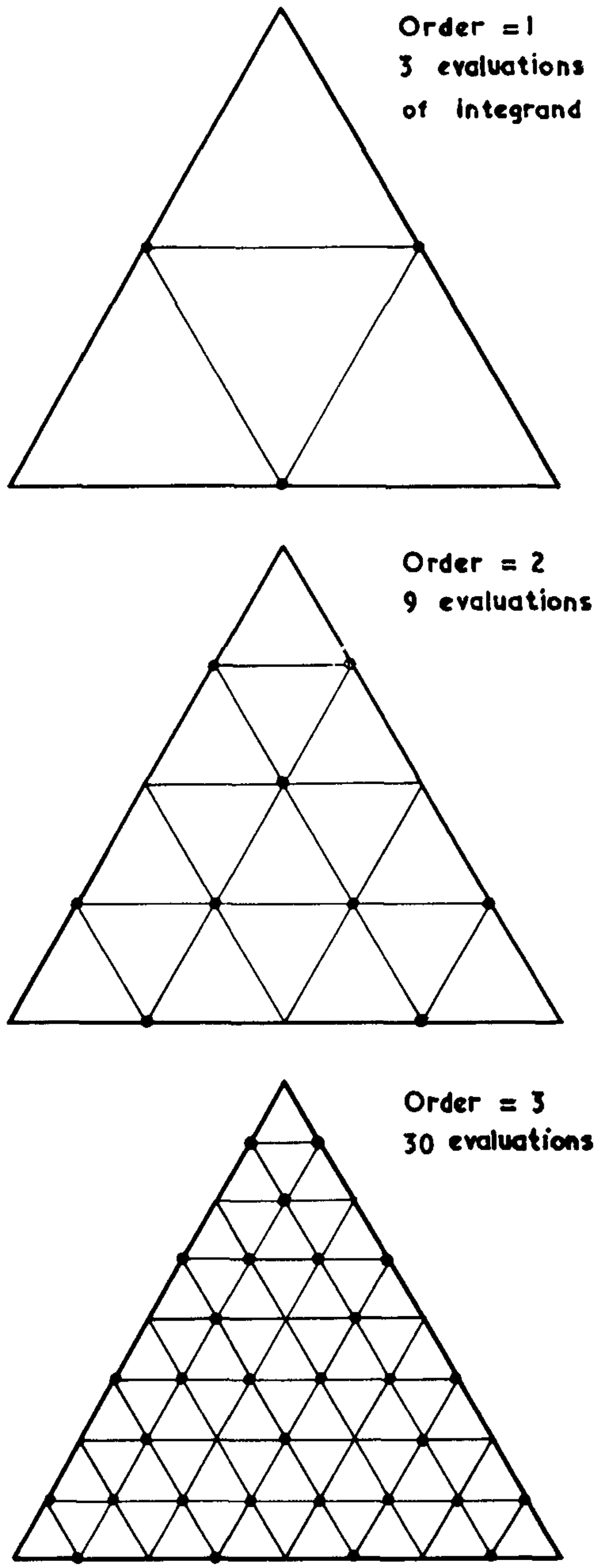

Integration over a triangle

FIG.10

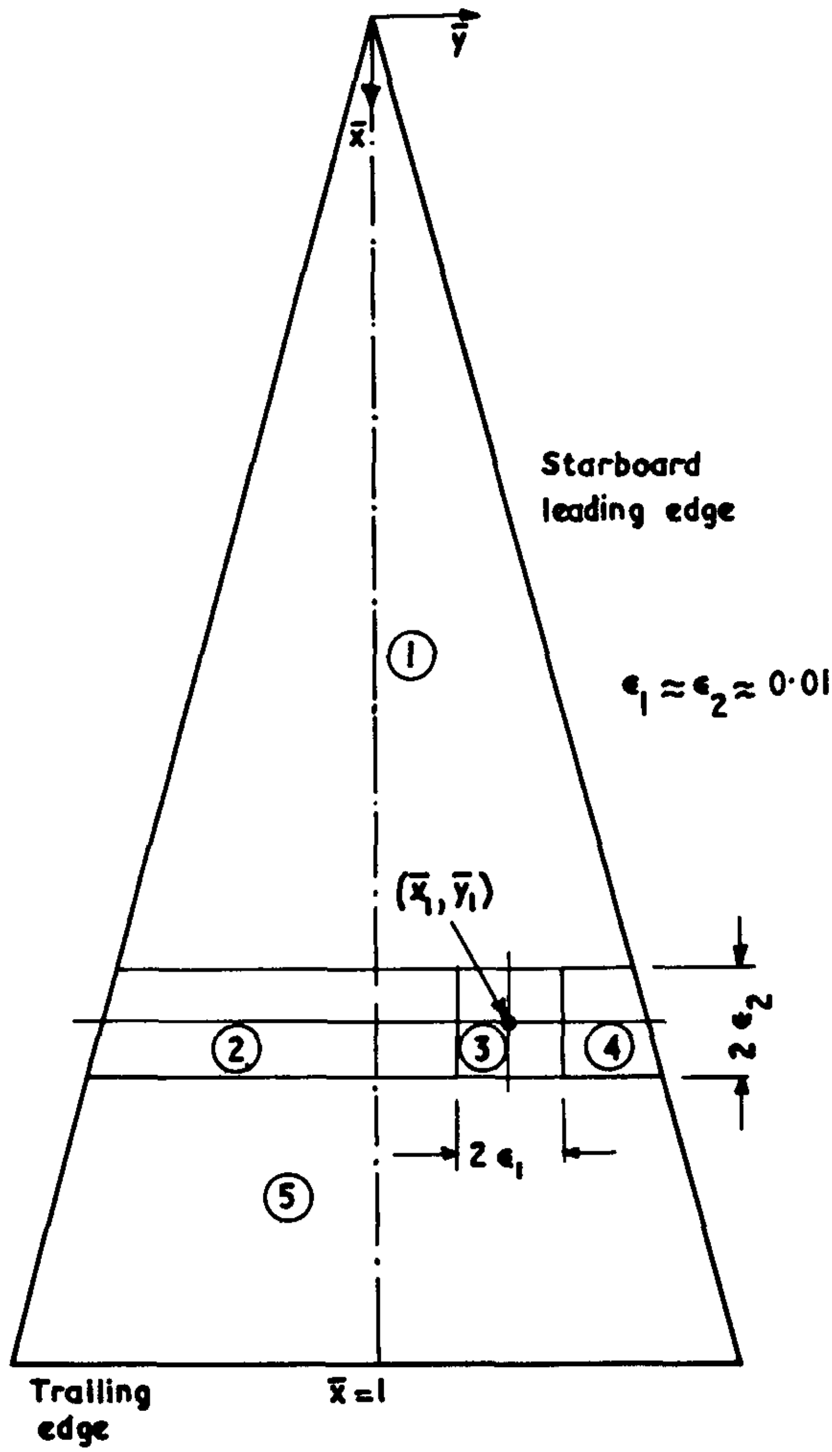

Regions of integration for upwash coefficients at point $(\bar{x}_1, \bar{y}_1)$

D 119319/1/144915 K.3 12/69 P

A.R.C. C.P. No.1086
August, 1968
Nangia, R. K. and Hancock, G. J.

A THEORETICAL INVESTIGATION FOR DELTA WINGS WITH LEADING-EDGE SEPARATION AT LOW SPEEDS

A non-linear lifting surface theory is postulated which incorporates the leading edge separations, by extending Brown and Michael's slender wing model, but satisfies the Kutta trailing edge condition. Results of a numerical application to a delta wing indicate acceptable trends compared with experimental data.

A.R.C. C.P. No.1086
August, 1968
Nangia, R. K. and Hancock, G. J.

A THEORETICAL INVESTIGATION FOR DELTA WINGS WITH LEADING-EDGE SEPARATION AT LOW SPEEDS

A non-linear lifting surface theory is postulated which incorporates the leading edge separations, by extending Brown and Michael's slender wing model, but satisfies the Kutta trailing edge condition. Results of a numerical application to a delta wing indicate acceptable trends compared with experimental data.

A.R.C. C.P. No.1086
August, 1968
Nangia, R. K. and Hancock, G. J.

A THEORETICAL INVESTIGATION FOR DELTA WINGS WITH LEADING-EDGE SEPARATION AT LOW SPEEDS

A non-linear lifting surface theory is postulated which incorporates the leading edge separations, by extending Brown and Michael's slender wing model, but satisfies the Kutta trailing edge condition. Results of a numerical application to a delta wing indicate acceptable trends compared with experimental data.

DETACHABLE ABSTRACT CARDS

C.P. No. 1086

Printed and published by
HER MAJESTY'S STATIONERY OFFICE

To be purchased from
49 High Holborn, London WC1
13a Castle Street, Edinburgh EH2 3AR
109 St Mary Street, Cardiff CF1 1JW
Brazennose Street, Manchester M60 8AS
50 Fairfax Street, Bristol BS1 3DE
258 Broad Street, Birmingham 1
7 Linenhall Street, Belfast BT2 8AY
or through any bookseller

Printed in England

C.P. No. 1086

SBN 11 470286 1